ARTICLES
https://doi.org/10.1038/s41593-019-0339-x
nature neuroscience

The DNA modification N6-methyl-2′-deoxyadenosine (m6dA) drives activity-induced gene expression and is required for fear extinction

Xiang Li[1,9*], Qiongyi Zhao[1,9], Wei Wei[1], Quan Lin[2], Christophe Magnan[3], Michael R. Emami[4,8], Luis E. Wearick-Silva[5], Thiago W. Viola[5], Paul R. Marshall[1], Jiayu Yin[1], Sachithrani U. Madugalle[1], Ziqi Wang[1], Sarah Nainar[6], Cathrine Broberg Vågbø[7], Laura J. Leighton[1], Esmi L. Zajaczkowski[1], Ke Ke[6], Rodrigo Grassi-Oliveira[5], Magnar Bjørås[7], Pierre F. Baldi[3], Robert C. Spitale[6] and Timothy W. Bredy[1*]

DNA modification is known to regulate experience-dependent gene expression. However, beyond cytosine methylation and its oxidated derivatives, very little is known about the functional importance of chemical modifications on other nucleobases in the brain. Here we report that in adult mice trained in fear extinction, the DNA modification N6-methyl-2′-deoxyadenosine (m6dA) accumulates along promoters and coding sequences in activated prefrontal cortical neurons. The deposition of m6dA is associated with increased genome-wide occupancy of the mammalian m6dA methyltransferase, N6amt1, and this correlates with extinction-induced gene expression. The accumulation of m6dA is associated with transcriptional activation at the brain-derived neurotrophic factor (Bdnf) P4 promoter, which is required for *Bdnf* exon IV messenger RNA expression and for the extinction of conditioned fear. These results expand the scope of DNA modifications in the adult brain and highlight changes in m6dA as an epigenetic mechanism associated with activity-induced gene expression and the formation of fear extinction memory.

In recent years, the understanding of neural plasticity, learning and memory has been advanced by the demonstration that various epigenetic processes are involved in the regulation of experience-dependent gene expression in the adult brain[1], and are critically involved in various forms of learning as well as the formation of fear extinction memory[2,3]. DNA methylation, once considered static and restricted to directing cellular lineage specificity during early development, is now recognized as being highly dynamic and reversible across the lifespan[4–6]. Although more than 20 DNA modifications have been identified[7], nearly all research aimed at elucidating the role of this epigenetic mechanism in the brain has focused on either 5-methylcytosine (5mC) or the recently rediscovered 5-hydroxymethycytosine (5hmC), which is a functionally distinct oxidated derivative of 5mC[8–10]. 5mC and 5hmC are highly prevalent in neurons relative to other cell types[8,11], and both modifications are regulated in response to learning under a variety of conditions, including the extinction of conditioned fear[2,12,13].

Beyond 5mC and 5hmC, N6-methyl-2'-deoxyadenosine (m6dA) is the most abundant DNA modification in prokaryotes where, in bacteria, m6dA regulates replication, transcription and transposition[14]. Until recently, m6dA had only been detected in unicellular eukaryotes[15,16]; however, due to notable technological improvements, it has now been shown to accumulate in a variety of eukaryotic genomes. For example, in *Chlamydomonas reindardtii*, m6dA is deposited at the transcription start site (TSS) and is associated with increased gene expression[17] and, in Drosophila, the level of m6dA increases across development and is enriched within transposable elements[18]. Furthermore, m6dA appears to be involved in reproductive viability and is associated with transgenerational mitochondrial stress adaptation in *Caenorhdoditis elegans*[19]. These observations have led to speculation that m6dA may play an important role in the regulation of gene expression across the lifespan. Several recent studies have extended these findings with the demonstration that m6dA is not only present in the mammalian genome[20–23], but is also highly dynamic and negatively correlates with LINE retrotransposon activity in both embryonic stem cells and in the brain of adult C57/Bl6 mice following exposure to chronic stress[20,24]. m6dA has also recently been shown to be enriched in gene bodies where it is positively associated with gene expression in human cell lines[20], yet little is known about the functional relevance of m6dA in specific neuronal populations in the mammalian brain, and a role for m6dA in the gene expression underlying learning and memory has yet to be reported.

The inhibition of learned fear is an evolutionarily conserved behavioral adaptation that is essential for survival. This process, known as fear extinction, involves the rapid reversal of the memory

[1]Cognitive Neuroepigenetics Laboratory, Queensland Brain Institute, The University of Queensland, Brisbane, Queensland, Australia. [2]Intellectual Development and Disabilities Research Center, David Geffen School of Medicine, University of California at Los Angeles, Los Angeles, CA, USA. [3]Department of Computer Science and Institute for Genomics and Bioinformatics, University of California Irvine, Irvine, CA, USA. [4]Department of Neurobiology and Behavior and Center for the Neurobiology of Learning and Memory, University of California Irvine, Irvine, CA, USA. [5]Brain Institute, Pontifical Catholic University of Rio Grande do Sul, Porto Alegre, Brazil. [6]Department of Pharmaceutical Sciences, University of California Irvine, Irvine, CA, USA. [7]Department of Cancer Research and Molecular Medicine, Norwegian University of Science and Technology, Trondheim, Norway. [8]Present address: Molecular Biology Institute, University of California Los Angeles, Los Angeles, CA, USA. [9]These authors contributed equally: Xiang Li, Qiongyi Zhao. *e-mail: x.li12@uq.edu.au; t.bredy@uq.edu.au

of previously learned contingencies and depends on gene expression in various brain regions, including the infralimbic prefrontal cortex (ILPFC). The model of fear extinction has long been recognized as an invaluable tool for investigating the neural mechanisms of emotional learning and memory, and the important contribution of the ILPFC to extinction has been demonstrated. A variety of epigenetic mechanisms in the ILPFC have been implicated in the extinction of conditioned fear[2,3,22] and this behavioral model provides a robust means of interrogating the role of epigenetic mechanisms in a critically important memory process. We therefore set out to explore the role of m6dA within the ILPFC and to elucidate whether it is involved in fear extinction.

Results

m6dA is dynamically regulated in response to neuronal activation. m6dA has recently been shown to be positively associated with transcription in lower eukaryotes[17] and humans[22]. We therefore hypothesized that m6dA may also be fundamental for governing activity-induced gene expression in differentiated neurons and in the adult brain. Three orthogonal approaches were used to establish the presence and dynamic nature of m6dA in cortical neurons (Fig. 1a). First, evidence was found in favor of m6dA as a modified base in neuronal DNA using a gel shift assay on genomic DNA derived from primary cortical neurons that had been treated with DpnI, a bacterially derived restriction enzyme that cuts double-stranded DNA specifically at methylated adenines, and predominantly within the GATC motif[17,23] (Fig. 1b and Supplementary Fig. 1a). We then performed liquid chromatography–tandem mass spectrometry (LC–MS/MS) to quantify the global level of m6dA within cortical neurons in response to neural activity. A standard KCl-induced depolarization protocol was used to induce neuronal activity in vitro[25], and a significant accumulation of m6dA was observed (Fig. 1c and Supplementary Fig. 1b). Finally, an immunoblot using an antibody that recognizes m6dA was used to verify the presence of m6dA following neuronal activation, again revealing a significant increase in m6dA (Fig. 1d). Together, these data demonstrate that m6dA is both a prevalent and inducible DNA modification in primary cortical neurons, findings that are in agreement with recent studies showing that m6dA is an abundant DNA modification in the mammalian genome[26], is responsive to stress[20] and is dynamically regulated in human disease states[27].

m6dA accumulates in the adult brain in response to extinction learning. Using activity-regulated cytoskeleton-associated protein (Arc) and a neuronal nuclear marker (NeuN) as tags for whole-cell fluorescence-activated cell sorting (FACS), we next enriched for a specific population of neurons in the mouse ILPFC that had been selectively activated by extinction learning (Supplementary Fig. 1a–c). The DpnI-seq approach[28] was then used to map the extinction learning-induced genome-wide accumulation of m6dA at single-base resolution, in vivo. As expected, we found that most m6dA sites cleaved by DpnI contain the motif GATC (Supplementary Fig. 2a,b), which is in line with previous reports[29,30]. Specifically, 2,033,704 G(m6dA)TC sites common to both extinction-trained (EXT) and retention control groups were detected, with 306,207 sites unique to the extinction training group and 212,326 sites unique to the retention control group (Fig. 2a). Overall, this represents 0.16% of total adenines and 30.49% of all GATCs in the mouse genome. This is notably more than a recent estimate of m6dA in human DNA derived from cell lines[24] where the predominant motif was [G/CAGG[C/T], and almost an order of magnitude larger than the estimate of differential m6dA regions in DNA derived from the mouse prefrontal cortex following exposure to chronic stress as assessed by m6dA-immunoprecipitation-seq[20], a discrepancy probably due to differences in the specific neuronal populations being investigated and the fact that Dpn1-seq is more sensitive than m6dA DIP-seq owing to its ability to provide information at base resolution. Alternating GATC sequences are abundant in eukaryotic DNA, have been estimated to account for nearly 0.5% of the total mammalian genome[31,32], and the GATC motif is frequently located at promoter regions where it has been shown to be directly associated with gene regulation[33–35]. Our data add to these

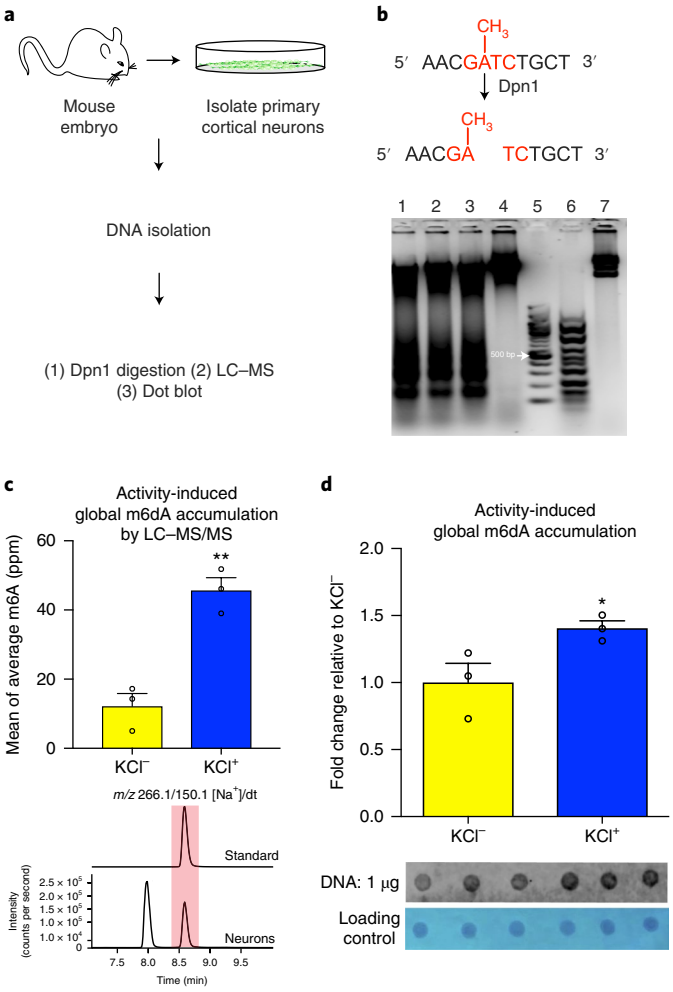

Fig. 1 | m6dA is present in the neuronal genome and accumulates in response to neural activation. a, Experimental plan to determine whether m6dA is a functionally relevant base modification in neurons. **b**, The Dpn1 enzyme cuts DNA specifically at methylated adenine in GATC linker sequences; Dpn1 digestion reveals the abundance of m6dA in DNA derived from primary cortical neurons, but not in DNA from liver (from the left; lanes 1–3: Dpn1-digested DNA from mouse primary cortical neurons, lane 4: Dpn1-digested DNA from mouse liver, lane 5: DNA ladder, lane 6: Dpn1-digested DNA from *Escherichia coli*, lane 7: undigested DNA from *E. coli*. **c**, LC–MS/MS detects a neuronal activity-induced global m6dA induction (7 DIV, 20 mM KCl, 7 h, two-tailed unpaired Student's *t*-test, $t = 6.411$, d.f. = 4, $^{**}P = 0.003$, median: $KCl^- = 12.17$ ppm; $KCl^+ = 45.63$ ppm). Representative LC–MS/MS chromatograms: control compound (m6dA standard) and isolated RNase-treated genomic DNA samples, which were extracted from primary cortical neurons, were used to directly quantify the global level of m6dA. **d**, Dot blot assay shows global accumulation of m6dA in stimulated primary cortical neurons (7 DIV, 20 mM KCl, 7 h, two-tailed unpaired Student's *t*-test, $t = 2.634$, d.f. = 4, $^{*}P = 0.02$, median: $KCl^- = 1$; $KCl^+ = 1.406$). For all panels, $n = 3$ biologically independent experiments per group; error bars represent s.e.m. Data distribution was assumed to be normal but this was not formally tested.

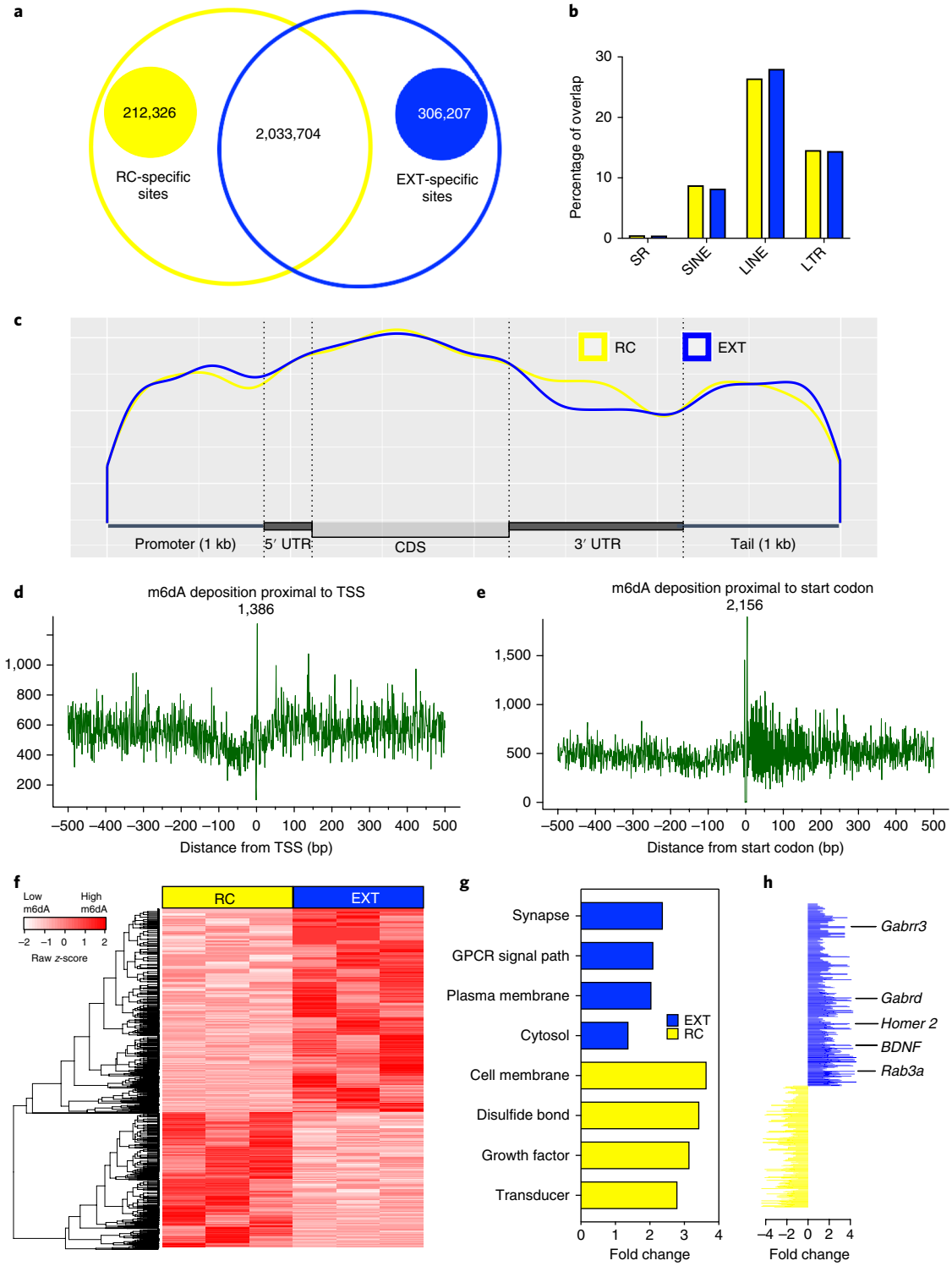

Fig. 2 | Experience-dependent redistribution of m6dA deposition within ILPFC neurons that have been activated by extinction learning. a, The Venn diagram shows the learning-induced increase in m6dA sites in retention control (RC) and EXT mice. **b**, There is no obvious difference with respect to the specific accumulation of m6dA from RC and EXT groups within repetitive elements. **c**, Metagene plot shows that m6dA deposition is primarily located in the promoter, 5′ UTR and CDS regions. **d**,**e**, Frequency plots demonstrating that m6dA is enriched at +1 bp from TSS (**d**) and exhibits a significant increase in deposition at +4 bp from the start codon (**e**). **f**, Representative heat map of genome-wide m6dA enrichment within active neurons after behavioral training (all $n = 3$ pooled samples per group; active neurons derived from five individual animals were pooled together). **g**, Gene ontology analysis of 10 gene clusters associated with m6dA deposition in RC versus EXT groups. **h**, Representative list of genes that exhibit a significant increase in the accumulation of m6dA and that have been associated with synaptic function, learning and memory.

observations and are the first to demonstrate that m6dA accumulates in neurons that have been selectively activated by fear extinction learning, further indicating that the dynamic accumulation of G(m6dA)TC may serve a critically important functional role in the epigenetic regulation of experience-dependent gene expression in the adult brain.

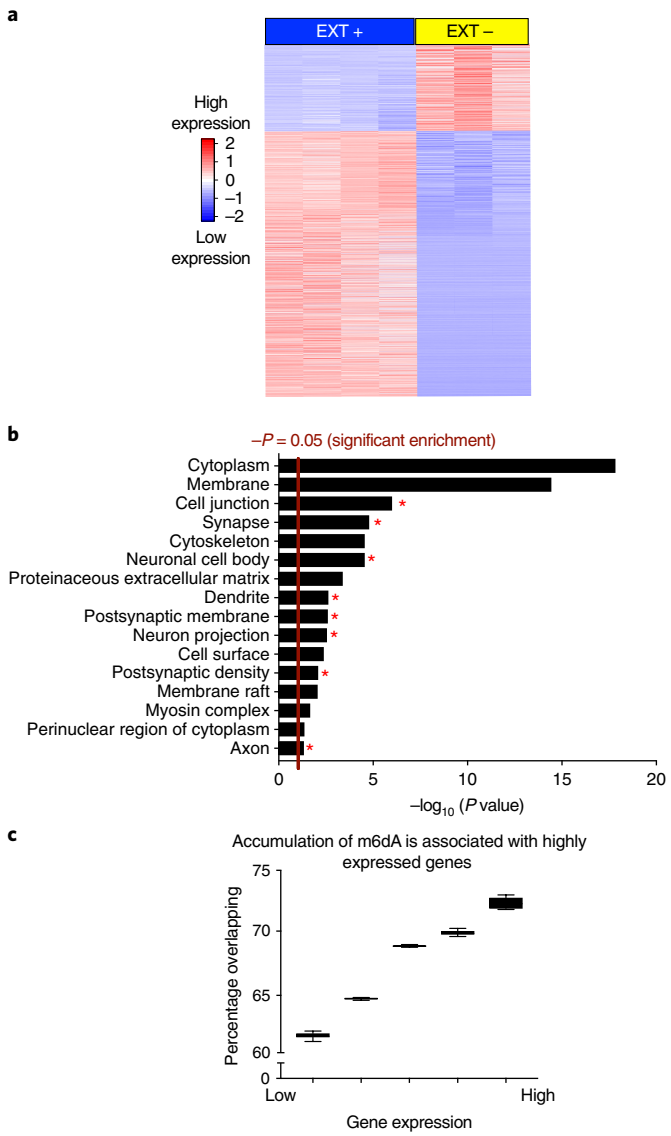

Fig. 3 | Extinction learning-induced accumulation of m6dA positively correlates with gene expression in activated neurons. a, Representative heat map of mRNA expression within activated neurons (EXT+) versus quiescent neurons (EXT−) ($n = 4$ biologically independent animals for EXT+; $n = 3$ individual animals for EXT−). **b**, Gene ontology analysis was carried out through the DAVID bioinformatic database. Gene ontology results show gene clusters enriched in the upregulated and differentially expressed genes; neuronal activity-related gene clusters are highlighted by red stars. **c**, Extinction learning-induced m6dA sites positively correlate with highly expressed genes ($n = 4$ biologically independent animals for EXT+ group; median for each group from expression low to high: 61.398, 64.445, 68.769, 69.844 and 72.297%).

It has been shown that chronic stress leads to the accumulation of m6dA within LINE1 elements in the adult prefrontal cortex[21]. Based on this observation, we next examined whether extinction learning-induced m6dA in activated neurons also overlaps with repeat elements across the genome, but found no relationship between the two (Fig. 2b). On the contrary, there was a significant effect of fear extinction learning on the accumulation of m6dA within the promoter, 5' untranslated region (UTR) and coding regions (CDS) (Fig. 2c). These findings are in accordance with previous studies identifying gene promoters and the transcription start site (TSS) as critical sites for the dynamic accumulation of m6dA[17,18,28], as well as the recent discovery of m6dA within coding regions of mammalian DNA[26]. A closer examination of the pattern of m6dA revealed a highly significant increase in the accumulation of m6dA at a site +1 bp downstream of the TSS (Fig. 2d) and a sharp increase in m6dA deposition +4 bp from the start codon (Fig. 2e). We also detected a significant difference in the experience-dependent accumulation of m6dA between EXT mice and retention controls (Fig. 2f). From a total of 2,839 differentially methylated m6dA sites, 1,774 GATC sites were specific to extinction, and a gene ontology analysis revealed that the most significant cluster specific to the extinction group was 'synapse' (Fig. 2g), with the top synapse-related genes that exhibited a significant accumulation of m6dA in response to extinction learning having previously been shown to be involved in learning and memory (Fig. 2h). Several of these candidates, including *Bdnf*, *Homer2*, *Gabrr3*, *Gabrd* and *Rab3a* were selected for validation. With the exception of the *Homer2* locus, we confirmed the Dpn1-seq data in an independent biological cohort by m6dA antibody capture followed by quantitative PCR (qPCR) from genomic DNA derived from total prefrontal cortex. (Fig. 5a and Supplementary Fig. 3). In a second independent biological cohort, we used DpnI treatment followed by qPCR, which is represented by a reduced PCR signal when there is more m6dA at a given locus. We found that a fear extinction learning-induced accumulation of m6dA occured at each of the selected candidate gene loci, including *Homer2*, but only in neurons that had been selectively activated by extinction training and not in quiescent neurons derived from the same brain region and from the same animals (Supplementary Fig. 4a–j). These data strongly indicate that extinction learning-induced m6dA accumulation is cell-type-specific and that this occurs in a highly state-dependent manner.

To further investigate the relationship between the dynamic accumulation of m6dA and cell-type-specific gene expression, RNA-seq was performed on RNA derived from activated and quiescent neurons immediately following fear extinction training. As expected, there was a general increase in gene expression within activated neurons, but not in quiescent neurons derived from the same brain region (Fig. 3a). A gene ontology analysis on extinction learning-induced genes again revealed significant extinction learning-related gene clusters, including 'synapse', 'dendrite' and 'postsynaptic membrane' (Fig. 3b), with a positive correlation between the accumulation of m6dA and gene expression in neurons selectively activated by fear extinction learning (Fig. 3c).

N6amt1 expression is activity-dependent and its deposition is associated with extinction learning-induced changes in m6dA. N6-adenine-specific DNA methyltransferase 1 (N6amt1) was originally described as a mammalian ortholog of the yeast adenine methyltransferase MTQ2. Homologs of N6amt1 have been shown to methylate N6-adenine in bacterial DNA[36], and mammalian N6amt1 has been shown to be a glutamine-specific protein methyltransferase[37]. N6amt1 is expressed in the mouse neocortex (http://mouse.brain-map.org/experiment/show?id=1234), as is N6amt2, with which it shares a highly conserved methyltransferase domain (http://mouse.brain-map.org/experiment/show?id=69837159). To obtain deeper insight into the underlying mechanism by which m6dA accumulates in the mammalian genome and regulates gene expression, we first examined the expression of N6amt1 and N6amt2 in primary cortical neurons in vitro and in the adult prefrontal cortex in response to fear extinction learning. *N6amt1* exhibited a significant increase in mRNA expression in primary cortical neurons in response to KCl-induced depolarization (Supplementary Fig. 5a), whereas there was no effect on *N6amt2* (Supplementary Fig. 5b). We next sought to determine whether the effects observed in primary cortical neurons also occur in the adult brain by examining *N6amt1* and *N6amt2* mRNA expression in the ILPFC in EXT mice relative to retention controls. Similar to the effect of KCl-induced

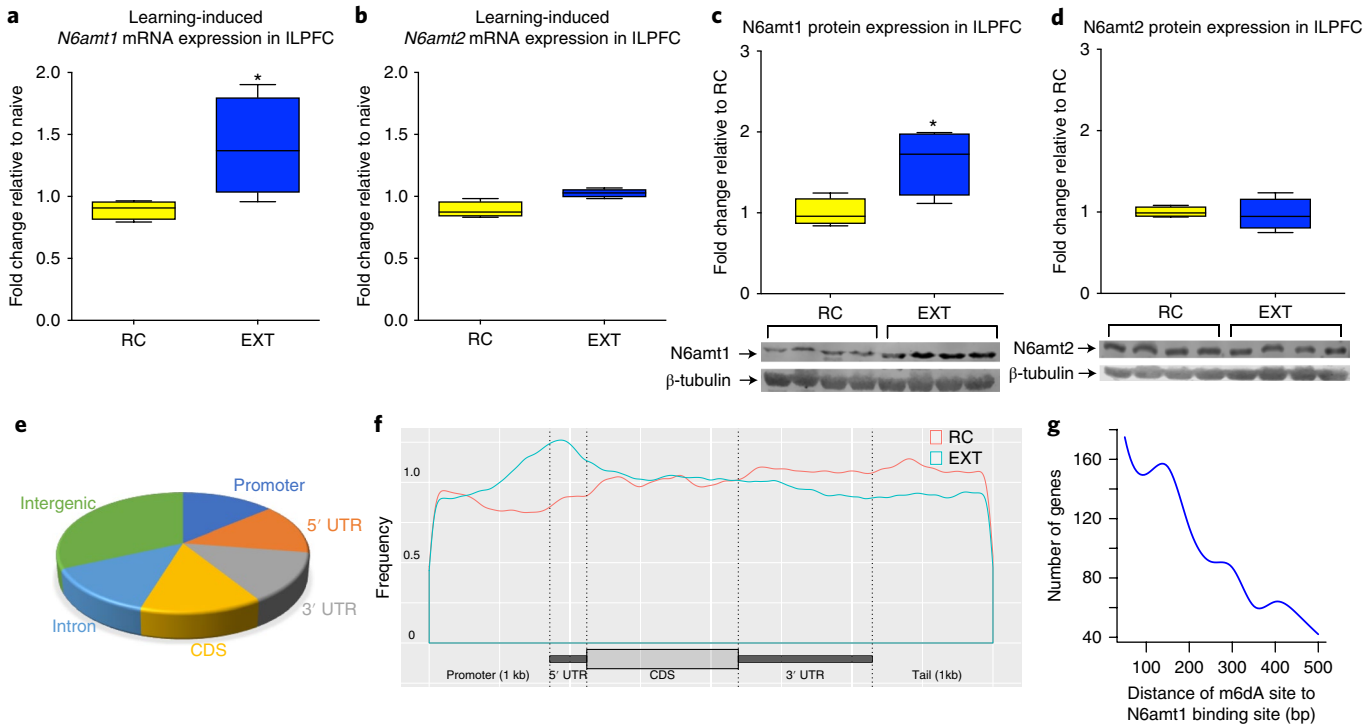

Fig. 4 | *N6amt1* mRNA expression is induced in the ILPFC in response to fear extinction learning, and N6amt1 occupancy increases within gene promoters and 5′ UTR. a, Extinction learning leads to increased expression of *N6amt1* in the ILPFC ($n=4$ biologically independent animals per group, two-tailed unpaired Student's *t*-test, $t=2.483$, d.f. = 6, $^*P=0.0476$, RC: median = 0.8931, data range 0.794–0.964 and EXT: median = 1.4, data range 0.957–1.902). **b**, No significant effect of learning on *N6amt2* mRNA expression in the ILPFC ($n=4$ biologically independent animals per group, two-tailed unpaired Student's *t*-test, $t=3.683$, d.f. = 6, $P=0.0609$, RC: median = 0.8906, data range 0.832–0.981 and EXT: median = 1.027, data range 0.982–1.068; data distribution was assumed to be normal but this was not formally tested). **c**,**d**, N6amt1 protein level is induced postextinction ($n=4$ biologically independent animals per group, two-tailed unpaired Student's *t*-test, $t=2.843$, d.f. = 6, $^*P=0.0295$, RC: median = 1, data range 0.829–1.244 and EXT: median = 1.64, data range 1.116–1.991, western blot image is cropped) (**c**) but not N6amt2 ($n=4$ biologically independent animals per group, two-tailed unpaired Student's *t*-test, $t=0.2906$, d.f. = 6, $P=0.7812$, RC: median = 1, data range 0.939–1.081 and EXT: median = 0.9691, data range 0.748–1.236, western blot image is cropped; data distribution was assumed to be normal but this was not formally tested) (**d**). **e**, Genome-wide N6amt1 distribution. **f**, Extinction training-induced increased in N6amt1 occupancy at promoter and 5′ UTR regions. **g**, There is a positive relationship between N6amt1 deposition and m6dA sites within promoter and 5′ UTR region, with more genes showing N6amt1 within 0–200 bp of m6dA sites.

depolarization on m6dA accumulation and *N6amt1* gene expression in vitro, fear extinction training led to a significant increase in *N6amt1* mRNA expression in the ILPFC (Fig. 4a), again with no detectable change in *N6amt2* (Fig. 4b). Moreover, there was also a concomitant increase in N6amt1 protein expression in the ILPFC (Fig. 4c and Supplementary Fig. 1c) with no effect on the level of N6amt2 (Fig. 4d and Supplementary Fig. 1d). Critically, the expression of N6amt1 was not induced in the ILPFC of mice that had received unpaired tone shock exposures during fear conditioning (pseudoconditioned) followed by strong extinction training (Supplementary Fig. 6a), indicating that *N6amt1* expression is engaged by extinction training and that it is a potentially important epigenetic modifier mediating the accumulation of m6dA in the adult brain in response to fear extinction learning.

To extend our understanding of the role of N6amt1 in fear extinction, we performed N6amt1 chromatin immunoprecipitation sequencing (ChIP-seq) on samples derived from the ILPFC of fear EXT mice. We found that although N6amt1 occupancy was equally distributed across genome (Fig. 4e), there was a significant increase in N6amt1 occupancy around gene promoters and 5′ UTR in response to fear extinction learning (Fig. 4f). We found 995 genes that exhibit both N6amt1 binding and accumulation of m6dA within ±500 bp of the TSS, which represents over 72% of the total genes that have m6dA sites specific for fear extinction (Supplementary Table 1). In addition, using a distance distribution plot, we observed that N6amt1 binding sites are proximal to m6dA sites in most genes (Fig. 4g). These findings indicate a functional relationship between an extinction learning-induced increase in N6amt1 occupancy and the accumulation of m6dA in the adult brain. However, the incomplete nature of the overlap between to the two datasets indicates that there are yet-to-be-identified epigenetic modifiers that contribute to the dynamic accumulation of m6dA and that these may be associated with other factors, such as the temporal dynamics of N6amt1 recruitment following learning. Indeed, recent work in *C. elegans* demonstrated that m6dA methyltransferase (DAMT-1) is required for transgenerational mitochondrial stress adaptation and permissive for mitochondrial gene expression[19]. Importantly, knockout of *damt-1* did not affect global levels of m6dA, indicating the existence of other adenine methyltransferases that could act in a cell-type-specific manner.

In an effort to establish a functional relationship between N6amt1 and the accumulation of m6dA in neuronal DNA, we next performed an *N6amt1* overexpression experiment on primary cortical neurons in vitro. Compared with a scrambled control, there was a global increase in m6dA within the cells that overexpressed the full length *N6amt1* (Supplementary Figs. 7a,b and 1e,f). Moreover, by knocking down *N6amt1* in vitro, we observed a reduction in the accumulation of m6dA (Supplementary Figs. 7c,d and 1g,h). These findings are in agreement with the recent demonstration of catalytically active N6amt1 in mammalian DNA, which was shown to

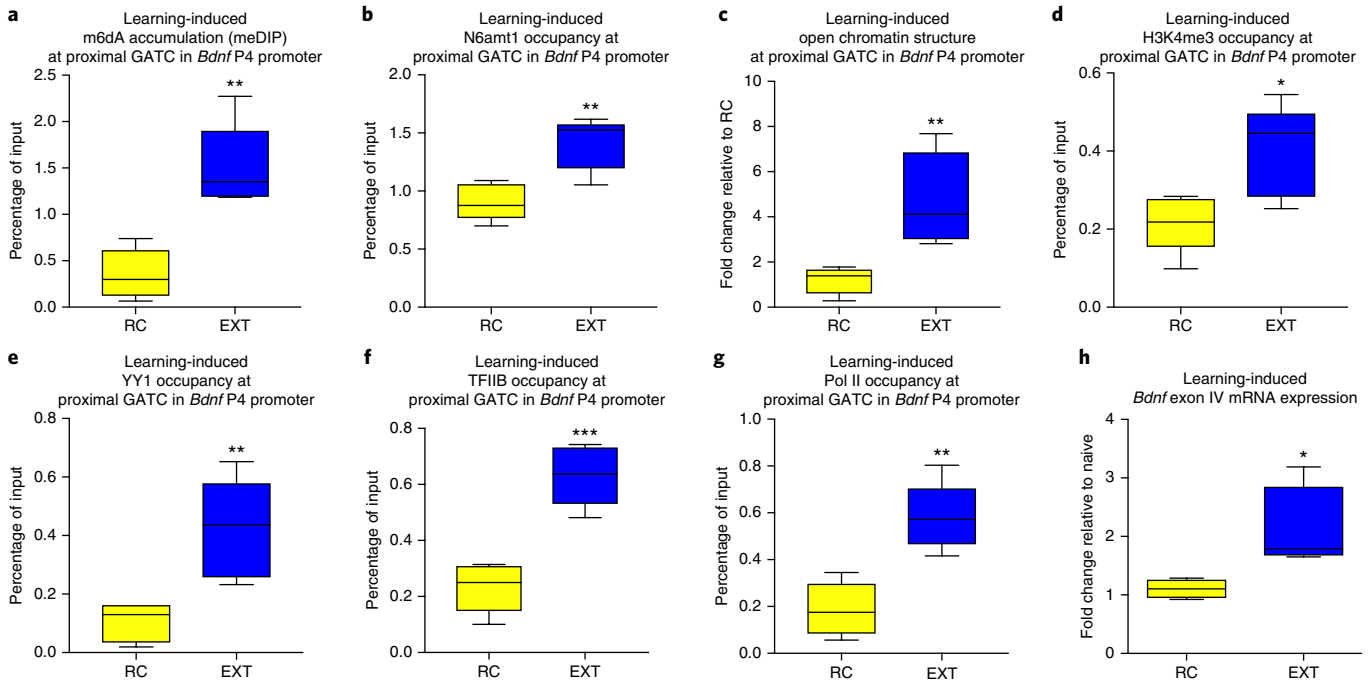

Fig. 5 | Extinction learning-induced accumulation of m6dA is associated with an active chromatin landscape and increased *Bdnf* exon IV mRNA expression. a–h, Fear extinction learning (EXT), relative to fear-conditioned mice exposed to a new context (RC), led to increased m6dA at the previously identified GATC site (two-tailed unpaired Student's *t*-test, $t = 4.921$, d.f. = 8, $^{**}P = 0.0012$, RC: median = 0.354, data range 0.065–0.739 and EXT: median = 1.506, data range 1.184–2.271) (**a**); a selective increase in N6amt1 occupancy (two-tailed unpaired Student's *t*-test, $t = 4.133$, d.f. = 8, $^{**}P = 0.0033$, RC: median = 0.9053, data range 0.699–1.089 and EXT: median = 1.412, data range 1.052–1.617) (**b**); an increased open chromatin structure, detected by using FAIRE-qPCR (two-tailed unpaired Student's *t*-test, $t = 3.76$, d.f. = 8, $^{**}P = 0.0055$, RC: median = 1.185, data range 0.282–1.780 and EXT: median = 4.771, data range 2.813–7.685) (**c**); a significant increase in $H3K4^{me3}$ occupancy (two-tailed unpaired Student's *t*-test, $t = 2.986$, d.f. = 8, $^{*}P = 0.0174$, RC: median = 0.2164, data range 0.098–0.284 and EXT: median = 0.400, data range 0.252–0.447) (**d**); an increase in the recruitment of YY1 (two-tailed unpaired Student's *t*-test, $t = 3.885$, d.f. = 8, $^{**}P = 0.0046$, RC: median = 0.1044, data range 0.019 to 0.162 and EXT: median = 0.4216, data range 0.232 to 0.652) (**e**); an increase in TFIIB occupancy (two-tailed unpaired Student's *t*-test, $t = 6.474$, d.f. = 8, $^{**}P = 0.0002$, RC: median = 0.2325, data range 0.100–0.314 and EXT: median = 0.6321, data range 0.579–0.742) (**f**); an increase in Pol II occupancy (two-tailed unpaired Student's *t*-test, $t = 4.838$, d.f. = 8, $^{**}P = 0.0013$, RC: median = 0.1873, data range 0.056–0.345 and EXT: medium = 0.5822, data range 0.416–0.803) (**g**); and a significant increase in *Bdnf* exon IV mRNA expression within the ILPFC (two-tailed unpaired Student's *t*-test, $t = 2.941$, d.f. = 8, $^{*}P = 0.0187$, RC: median = 0.1.104, data range 0.922–1.285 and EXT: median = 2.104, data range 1.650–3.188) (**h**). In all panels, $n = 5$ biologically independent animals per group; data distribution was assumed to be normal but this was not formally tested.

be necessary for the conversion of adenine to m6dA under both synthetic conditions and in human cell lines[26]. Importantly, in that study, N6amt1 had no effect on the acccumulation of RNA m6A, therefore confirming a functional role for N6amt1 as a bona fide mammalian DNA adenine methyltransferase. In contrast, Xie et al.[27] did not detect N6amt1 methyltransferase activity on DNA derived from glioblastoma cells, further indicative of the possibility of a cell-type-specific role for N6amt1 that may rely on yet to be indentified epigenetic cofactors.

Extinction learning-induced N6amt1-mediated accumulation of m6dA drives *Bdnf* exon IV mRNA expression in the ILPFC. Bdnf is the most widely expressed inducible neurotrophic factor in the central nervous system[38] and is directly involved in extinction-related learning and memory[39]. In the adult brain, the accumulation of 5mC within *Bdnf* gene promoters is altered by experience[40], and this epigenetic mechanism is necessary for the regulation of gene expression underlying remote memory[12]. The *Bdnf* locus comprises at least eight homologous noncoding exons that contribute to alternate 5′ UTRs and a ninth that contributes a protein coding sequence and 3′ UTR. The complex structure of this genomic locus has led to the idea that *Bdnf* mRNA expression may be driven by DNA modifications that guide distinct sets of transcription factor complexes to initiate the transcription of the various isoforms[41], all of which could be important for learning and memory. This is supported by the fact that exon IV is highly activity-dependent and plays a direct role in the formation of fear extinction memory[22,42].

There was a highly specific accumulation of m6dA at a GATC site immediately downstream of the TSS of the *Bdnf* P4 promoter in fear EXT mice, an effect not observed in in pseudoconditioned control mice (Fig. 5a and Supplementary Figs. 4a and 6b). DNA immunoprecipitation analysis using an m6dA-specific antibody confirmed that extinction training led to an increase of m6dA at this locus and that this signal could be detected within a mixed homogenate derived from the ILPFC of EXT mice (Fig. 5a). Adjacent to this GATC site is a N6amt1 binding site (Supplementary Table 1), supporting the idea that the accumulation of m6dA is mediated by N6amt1. To further investigate this possibility, we used chromatin immunoprecipitation followed by qPCR (ChIP–qPCR) to detect occupancy of N6amt1 at this genomic locus following extinction training. We found an increase in N6amt1 occupancy at this genomic locus in EXT (Fig. 5b) but not pseudoconditioned control mice (Supplementary Fig. 6c), which further indicates an intimate relationship between extinction learning-induced N6amt1 occupancy and the accumulation of m6dA. This is the only GATC site found within 500 bp of the TSS of *Bdnf* exon IV, which again indicates a high amount of selectivity

with respect to where and when m6dA dynamically accumulates in the genome in response to extinction training. To reveal the chromatin status, we applied formaldehyde-assisted isolation of regulatory elements (FAIRE) following qPCR[43] and found increased activity at this m6dA-modified GATC site (Fig. 5c), which, when considered in conjunction with the deposition of H3K4me^3 (Fig. 5d), further indicates a functionally relevant relationship between m6dA and the induction of an open chromatin state. There is a consensus sequence for the activating transcription factor Yin-Yang (YY1)[21] adjacent to the m6dA site, and fear extinction learning led to a significant increase in the recruitment of YY1 (Fig. 5e), as well as in elements of the transcriptional machinery, including TFIIB (Fig. 5f) and Pol II (Fig. 5g). The activity-induced changes in N6amt1 occupancy, m6dA accumulation and related effects on the local chromatin landscape and transcriptional machinery strongly correlated with increased *Bdnf* exon IV mRNA expression specifically in response to fear extinction training (Fig. 5h), with no effect of extinction training on *Bdnf* exon IV mRNA expression in pseudo-conditioned control mice (Supplementary Fig. 6d). There was also no effect in IgG controls (Supplementary Fig. 8a–f) at a distal GATC motif located 1,000 bp upstream of TSS (Supplementary Fig. 9a–f), or proximal to TSS in the *Bdnf* P1 promoter (Supplementary Fig. 10a–h). The proximal promoter region of another plasticity-related gene, *Rab3a*, also exhibited a pattern of epigenetic modification similar to that of *Bdnf* P4 locus and a subsequent increase in gene expression in response to fear extinction learning (Supplementary Fig. 11a–f), which further indicates a generalized role for m6dA in the epigenetic regulation of experience-dependent gene expression in the adult brain.

N6amt1-mediated accumulation of m6dA is associated with increased gene expression and the formation of fear extinction memory. Having established a relationship between the fear extinction learning-induced accumulation of m6dA and the regulation of *Bdnf* exon IV mRNA expression in vivo, we next investigated whether lentiviral-mediated knockdown of *N6amt1* in the ILPFC affects the formation of fear extinction memory. We first validated the efficiency of the knockdown construct in vivo, which showed excellent transfection efficiency and a reliable decrease in *N6amt1* mRNA expression within viral-infected neurons after infused directly into the ILPFC before behavioral training (Fig. 6a,b and Supplementary Fig. 12). There was no effect of *N6amt1* short hairpin RNA (shRNA) on within-session performance during the first 15 conditioned stimulus exposures during fear extinction training (Fig. 6c,d), and there was no effect of *N6amt1* shRNA on fear expression in mice that had been fear-conditioned and exposed to a new context without extinction training (Fig. 6e, left). However, there was a highly significant impairment in fear extinction memory in mice that had been extinction trained in the presence of *N6amt1* shRNA (Fig. 6e, right). Infusion of *N6amt1* shRNA into the prelimbic region of the prefrontal cortex, a brain region immediately dorsal to the ILPFC, had no effect on extinction memory (Supplementary Fig. 13a–c). These data indicate a critical role for the N6amt1-mediated accumulation of m6dA in the ILPFC in regulating the formation of fear extinction memory as opposed to generalized negative effects on fear-related learning and memory.

To draw stronger conclusions about the relationship between m6dA, *Bdnf* mRNA expression and extinction memory, we next asked whether a direct application of recombinant Bdnf into the ILPFC before extinction training could rescue the impairment of extinction memory associated with N6amt1 knockdown. In the presence of *N6amt1* shRNA, Bdnf-treated mice exhibited a significant reduction in freezing relative to saline-infused mice during extinction training (Fig. 6f–h), which indicates a causal relationship between N6amt1-mediated accumulation of m6dA, *Bdnf* exon IV expression and the formation of fear extinction memory. With respect to the epigenetic landscape and transcriptional machinery surrounding the *Bdnf* P4 promoter, knockdown of *N6amt1* prevented the fear extinction learning-induced increase in *N6amt1* expression (Supplementary Fig. 14) and occupancy (Fig. 7a) and the accumulation of m6dA (Fig. 7b). *N6amt1* knockdown also blocked the fear extinction learning-induced change in chromatin state (Fig. 7c), as well as the previously observed increases in H3K4^{me3} (Fig. 7d),

Fig. 6 | N6amt1-mediated accumulation of m6dA is required for fear extinction memory and for learning-induced *Bdnf* exon IV mRNA expression in the ILPFC. a, Left: representative image of cannula placement in the ILPFC, right: transfection of *N6amt1* shRNA into the ILPFC. **b**, *N6amt1* mRNA expression analysis in non-FACS and FACS-sorted cells. A significant reduction of *N6amt1* expression was only observed in FACS-sorted cells ($n = 5$ biologically independent animals per group. Non-FACS-sorted groups: two-tailed unpaired Student's *t*-test, $t = 1.559$, d.f. = 8, RC: mean = 0.861, data range 0.461–1.211 and EXT: mean = 1.709, data range 0.936–1.289. FACS-sorted groups: two-tailed unpaired Student's *t*-test, $t = 4.956$, d.f. = 8, $^{**}P = 0.0011$, RC: mean = 1.128, data range 0.671–1.510 and EXT: mean = 0.2537, data range 0.105–0.537). **c**, Schematic of the behavioral protocol used to test the effect of lentiviral-mediated knockdown of N6amt1 in the ILPFC on fear extinction memory. CTX, context; CS, conditioned stimulus; US, unconditioned stimulus. **d**, There was no effect of *N6amt1* shRNA on within-session performance during the first 15 conditioned stimulus exposures during fear extinction training ($n = 8$ biologically independent animals per group, two-way ANOVA, $F_{1,210} = 2.539$, $P = 0.1126$; Bonferroni's post hoc test, all $P > 0.9999$). **e**, Although there was no effect of *N6amt1* shRNA on fear expression in mice that had been fear conditioned and exposed to a new context without extinction training, N6amt1 knockdown led to a significant impairment in fear extinction memory ($n = 8$ biologically independent animals per group, two-way ANOVA, $F_{1,28} = 16.9$, $P < 0.0001$; Dunnett's post hoc test: scrambled control RC versus scrambled control EXT, $^{**}P = 0.0019$, scrambled control RC: median = 40.21, data range 13.56–63.78; shRNA RC: median = 46.13, data range 34.00–64.81; scramble control EXT: median = 10.57, data range 0.00–32.07; shRNA EXT: median = 49.68, data range 30.29–85.75). **f**, Schematic of the behavioral protocol used to test the effect of BDNF injection within N6amt1-knockdown animals on fear extinction memory. **g**,**h**, ILPFC infusion of BDNF has minimum effect during extinction training ($n = 5$ biologically independent animals per group, two-way ANOVA, $F_{1,120} = 105$, $P < 0.0001$; Bonferroni's post hoc test: *N6amt1* shRNA + saline versus N6amt1 + BDNF section 4: $^{*}P = 0.0121$; *N6amt1* shRNA + saline: median = 67.2, data range 38.56–95.33; and N6amt1 + BDNF: median = 19.78, data range 3.67–40.22; section 10: $^{**}P = 0.0033$; *N6amt1* shRNA + saline: median = 74.87, data range 26.22–98.89; and N6amt1 + BDNF: median = 22.27, data range 11.00–26.67; section 11: $^{**}P = 0.0022$; *N6amt1* shRNA + saline: median = 67.41, data range 10.21–96.67; and N6amt1 + BDNF: median = 13.27, data range 2.44–19.20; section 12: $^{**}P = 0.0092$; *N6amt1* shRNA + saline: median = 68.78, data range 10.44–91.33; and N6amt1 + BDNF: median = 20.2, data range 9.99 –60.82; section 13: $^{**}P = 0.0035$; *N6amt1* shRNA + saline: median = 76.58, data range 54.16–96.89; and N6amt1 + BDNF: median = 24.26, data range 9.99–60.82; section 14: $^{*}P = 0.0429$; *N6amt1* shRNA + saline: median = 71.47, data range 19.56–97.78 and N6amt1 + BDNF: median = 29.44, data range 2.11–48.67; and section 15: $^{*}P = 0.0254$; *N6amt1* shRNA + saline: median = 74.38, data range 39.29–95.12; and N6amt1 + BDNF: median = 30.06, data range 7.44–62.15) (**g**), and promotes extinction or rescues the *N6amt1* shRNA-induced impairment in fear extinction memory ($n = 5$ biologically independent animals per group, two-way ANOVA, $F_{1,17} = 13.38$, $P < 0.01$; Dunnett's post hoc test: *N6amt1* shRNA + saline versus N6amt1 + BDNF, $^{**}P = 0.0052$, *N6amt1* shRNA + saline RC: median = 48.82, data range 24.86–67.76; N6amt1 + BDNF RC: median = 57.16, data range 26.04–73.64; *N6amt1* shRNA + saline EXT: median = 43.54, data range 35.96–57.16; N6amt1 + BDNF EXT: median = 13.107, data range 4.05–22.11) (**h**). Data distribution was assumed to be normal but this was not formally tested.

YY1 (Fig. 7e), TFIIB (Fig. 7f) and Pol II (Fig. 7g) recruitment to the *Bdnf* P4 promoter. Finally, *N6amt1* knockdown prevented the fear extinction learning-induced increase in *Bdnf* exon IV mRNA expression (Fig. 7h). Taken together, these findings indicate that, in the ILPFC, dynamic, learning-induced accumulation of m6dA is necessary for epigenetic regulation of experience-dependent *Bdnf* exon IV expression and is critically involved in the formation of fear extinction memory.

Discussion

Although more than 20 different base modifications are known to occur in DNA[7], only 5mC and 5hmC have been studied in any detail

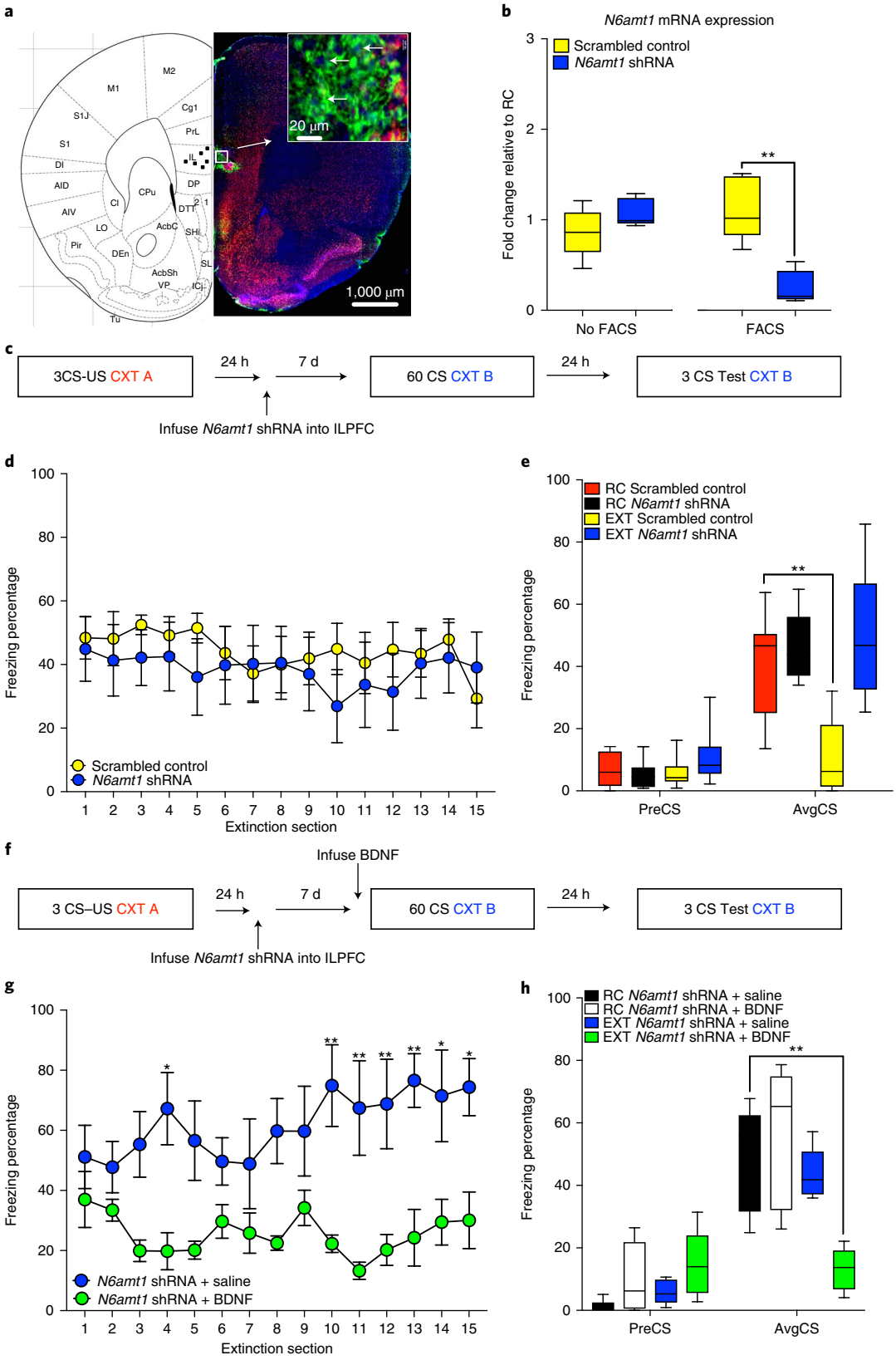

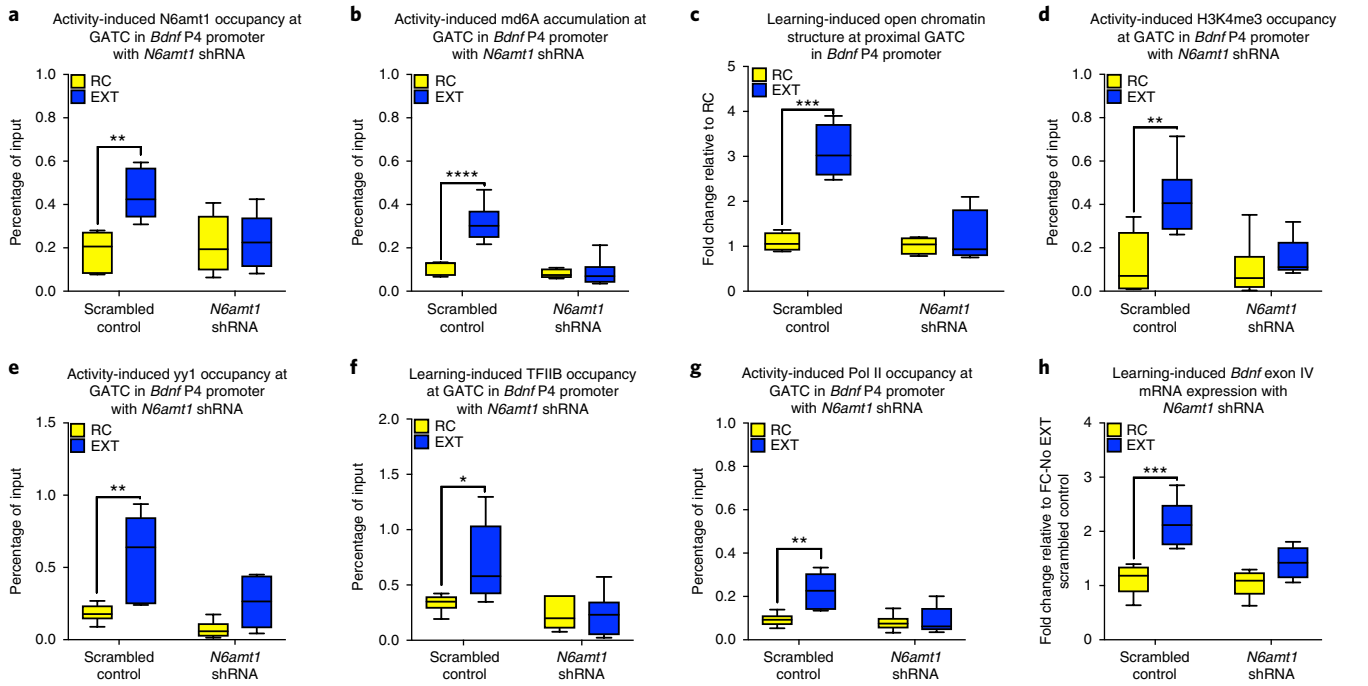

Fig. 7 | N6amt1 knockdown prevents the learning-induced accumulation of m6dA and related changes in chromatin and transcriptional landscape associated with the *Bdnf* P4 promoter. a–g, *N6amt1* shRNA blocked the learning-induced increase in N6amt1 occupancy ($n=6$ biologically independent animals per group, two-way ANOVA, $F_{1,20}=7.663$, $P<0.05$; Dunnett's post hoc test: scrambled control RC versus scrambled control EXT, $^{**}P=0.0041$, scramble control RC: median = 0.187, data range 0.082–0.280; scramble control EXT: median = 0.444, data range 0.308–0.594) (**a**) and the deposition of m6dA ($n=5$ biologically independent animals in the RC scramble control group; $n=6$ biologically independent animals per group for all other groups, two-way ANOVA, $F_{1,19}=18.56$, $P<0.0001$; Dunnett's post hoc test: scrambled control RC versus scrambled control EXT, $^{****}P<0.0001$, scrambled control RC: median = 0.107, data range 0.066–0.133; scrambled control EXT: median = 0.314, data range 0.217–0.468) (**b**) or open chromatin structure ($n=4$ biologically independent animals per group, two-way ANOVA, $F_{1,12}=19.38$, $P<0.001$; Dunnett's post hoc test: scrambled control RC versus scrambled control EXT, $^{***}P=0.0001$, scrambled control RC: median = 1.089, data range 0.866–1.365; scrambled control EXT: median = 3.103, data range 2.478–3.901) (**c**); the accumulation of H3K4me^3 ($n=6$ biologically independent animals per group, two-way ANOVA, $F_{1,20}=9.815$, $P<0.01$; Dunnett's post hoc test: scrambled control RC versus scrambled control EXT, $^{**}P=0.0046$, scrambled control RC: median = 0.126, data range 0.008–0.342; scrambled control EXT: median = 0.421, data range 0.261–0.714) (**d**); YY1 ($n=6$ biologically independent animals per group, two-way ANOVA, $F_{1,20}=17.64$, $P<0.001$; Dunnett's post hoc test: scrambled control RC versus scrambled control EXT, $^{**}P=0.0018$, scrambled control RC: median = 0.183, data range 0.088–0.268; scrambled control EXT: median = 0.587, data range 0.240–0.814) (**e**); induction of TFIIB occupancy ($n=6$ biologically independent animals per group, two-way ANOVA, $F_{1,20}=10.03$, $P<0.01$; Dunnett's post hoc test: scrambled control RC versus scrambled control EXT, $^{*}P=0.0258$, scrambled control RC: median = 0.335, data range 0.191–0.421; scrambled control EXT: median = 0.699, data range 0.347–1.296) (**f**) and RNA Pol II ($n=6$ biologically independent animals per group, two-way ANOVA, $F_{1,20}=8.883$, $P<0.01$; Dunnett's post hoc test: scrambled control RC versus scrambled control EXT, $^{**}P=0.0024$, scrambled control RC: median = 0.092, data range 0.075–0.139; scrambled control EXT: median = 0.226, data range 0.134–0.296) occupancy at the proximal GATC site within the *Bdnf* P4 promoter (**g**). **h**, *N6amt1* shRNA also inhibited *Bdnf* exon IV mRNA expression ($n=5$ biologically independent animals per group, two-way ANOVA, $F_{1,16}=20.95$, $P<0.001$; Dunnett's post hoc test: scrambled control RC versus scrambled control EXT, $^{***}P=0.0007$, scrambled control RC: median = 1.127, data range 0.638–1.396; scrambled control EXT: median = 2.117, data range 1.683–2.850). Data distribution was assumed to be normal but this was not formally tested.

within the adult brain. Here we provide evidence that the learning-induced accumulation of m6dA in post-mitotic neurons is associated with an increase in gene expression and is required for the formation of fear extinction memory. m6dA has emerged as a functionally relevant DNA modification that is commonly found in bacterial DNA and lower eukaryotes[15,16,29,30,44,45]. m6dA is abundant in the mammalian genome[21,22,26] and its accumulation in the prefrontal cortex is associated with chronic stress[20]. We have now extended these observations and provide strong evidence for a global induction of m6dA in response to neuronal activation, which is accompanied by an activity-dependent increase in the expression of the m6dA methyltransferase N6amt1. This is critically involved in the extinction learning-induced accumulation of m6dA at the *Bdnf* P4 promoter and in the extinction of conditioned fear. Strikingly, the effect of experience on m6dA accumulation occurs only in neurons that have been activated by training and not in quiescent neurons from the same brain region. These data therefore indicate that neurons use m6dA as an epigenetic regulatory mechanism that is engaged specifically under activity-induced conditions and that this is mediated by the action of N6amt1. Whether m6dA has similar regulatory control over experience-dependent gene expression in other cell types and in other regions of the brain remains to be determined.

As indicated, overexpression of *N6amt1* led to a global increase in m6dA within primary cortical neurons and led to a positive correlation between N6amt1 occupancy and the level of m6dA, similar to the recent demonstration of catalytically active N6amt1 mediating the accumulation of m6dA in human DNA[26]. However, as indicated by our genome-wide profiling study, N6amt1 binding did not show complete overlap with sites of extinction learning-induced m6dA accumulation within gene promoters. Therefore, it is likely that, to confer temporally regulated changes in the accumulation of m6dA in cortical neurons, N6amt1 must also work in complex with other factors. Future studies will determine the full repertoire of proteins and RNA that are required to direct N6amt1 to sites of action on DNA in an experience- or activity-dependent manner.

It is noteworthy that the fear extinction learning-induced accumulation of m6dA was prominent not only around the TSS, but also along the CDS, which shows a similar pattern in the human genome[26]. Notably, previous work has shown that m6dA is associated with Pol II-transcribed genes[46], and the accumulation of m6dA in exons positively correlates with gene transcription[26]. Together with our data, these findings indicate that m6dA may play an important role in initiating transcription by promoting an active chromatin state and, with the recruitment of Pol II, may contribute to the efficiency of Pol II read-through along the gene body. We found that highly expressed genes tend to have more m6dA in their promoter regions. m6dA has also been shown to overlap with nucleosome-free regions[17], which serve to facilitate transcription elongation. This indicates an essential role for the deposition of m6dA along the CDS in regulating learning-induced transcriptional processes, which is required for the underlying changes in gene expression that accompany the formation of fear extinction memory. Future studies will examine the direct relationship between the dynamic accumulation of m6dA and DNA structure states, as well as their influence on gene expression and on other forms of learning and memory.

Our data indicate that there is positive relationship between the accumulation of m6dA and gene expression within neurons in ILPFC that have been activated by extinction learning. Moreover, we have discovered that activity-induced expression of *Bdnf* exon IV in the ILPFC following behavioral training is functionally related to an N6amt1-mediated increase in the accumulation of m6dA at the *Bdnf* P4 promoter. This is associated with an open chromatin structure as well as the presence of H3K4me3, an epigenetic mark that reflects an active chromatin state. It is also accompanied by increased recruitment of the transcription factors YY1 and TFIIB, as well Pol II, to the same locus. Thus, these findings demonstrate that the accumulation of m6dA surrounding the TSS of the *Bdnf* P4 promoter drives activity-induced and experience-dependent exon IV mRNA expression. Recent studies in whole-cell homogenates have indicated a repressive function of m6dA accumulation under stress in rodents and in human embryonic stem cells and in glioblastoma[20,27,47], which is in stark contrast to our finding of a permissive role for m6dA accumulation and experience-dependent gene expression. We have previously found that the pattern of 5mC within the adult brain differs in neurons and non-neuronal cells and that 5hmC exhibits a dramatic redistribution in the adult ILPFC in response to fear extinction learning[2,48]. Together, these lines of evidence indicate that learning-induced changes in DNA modification may be both dynamic and cell-type-specific, with the current findings supporting this conclusion. Our findings on a positive relationship between m6dA and gene expression are also supported by the recent discovery of a mitochondrial-specific adenine methyltransferase that is required for mitochondrial stress adaptation and drives mitochondrial gene expression[19]. Thus, the context- and state-dependent role of m6dA in specific cell types deserves further consideration as an important epigenetic mechanism of experience-dependent gene regulation, and future studies will expand this analysis in the brain in response to different forms of learning and memory.

In summary, we have shown that the N6amt1-mediated accumulation of m6dA is dynamically regulated in the mammalian genome and that its deposition drives activity-induced *Bdnf* exon IV mRNA expression and is required for the extinction of conditioned fear. Our findings indicate a model where, in selectively activated neurons in the adult brain, the accumulation of m6dA serves as a permissive epigenetic signal for the regulation of activity- or learning-induced gene expression (Supplementary Fig. 15). These results expand the scope of experience-dependent DNA modifications in the brain and strongly indicate that the information-processing capacity of DNA in post-mitotic neurons is far more complex than current perspectives generally appreciate. We predict that a large number of functional modifications on all four canonical nucleobases, with diverse roles in the epigenetic regulation of experience-dependent gene expression, learning and memory, remain to be discovered.

Online content

Any methods, additional references, Nature Research reporting summaries, source data, statements of data availability and associated accession codes are available at https://doi.org/10.1038/s41593-019-0339-x.

Received: 24 July 2018; Accepted: 10 January 2019;
Published online: 18 February 2019

References

1. Marshall, P. & Bredy, T. W. Cognitive neuroepigenetics: the next evolution in our understanding of the molecular mechanisms underlying learning and memory? *NPJ Sci. Learn.* **1**, 16014 (2016).
2. Li, X. et al. Neocortical Tet3-mediated accumulation of 5-hydroxymethylcytosine promotes rapid behavioral adaptation. *Proc. Natl Acad. Sci. USA* **111**, 7120–7125 (2014).
3. Wei, W. et al. p300/CBP-associated factor selectively regulates the extinction of conditioned fear. *J. Neurosci.* **32**, 11930–11941 (2012).
4. Miller, C. A., Campbell, S. L. & Sweatt, J. D. DNA methylation and histone acetylation work in concert to regulate memory formation and synaptic plasticity. *Neurobiol. Learn. Mem.* **89**, 599–603 (2008).
5. Baker-Andresen, D., Ratnu, V. S. & Bredy, T. W. Dynamic DNA methylation: a prime candidate for genomic metaplasticity and behavioral adaptation. *Trends Neurosci.* **36**, 3–13 (2013).
6. Gapp, K., Woldemichael, B. T., Bohacek, J. & Mansuy, I. M. Epigenetic regulation in neurodevelopment and neurodegenerative diseases. *Neuroscience* **264**, 99–111 (2014).
7. Korlach, J. & Turner, S. W. Going beyond five bases in DNA sequencing. *Curr. Opin. Struct. Biol.* **22**, 251–261 (2012).
8. Lister, R. et al. Global epigenomic reconfiguration during mammalian brain development. *Science* **341**, 1237905 (2013).
9. Guo, J. U., Su, Y., Zhong, C., Ming, G.-L. & Song, H. Hydroxylation of 5-methylcytosine by TET1 promotes active DNA demethylation in the adult brain. *Cell* **145**, 423–434 (2011).
10. Shen, L. et al. Tet3 and DNA replication mediate demethylation of both the maternal and paternal genomes in mouse zygotes. *Cell Stem Cell* **15**, 459–471 (2014).
11. Khare, T. et al. 5-hmC in the brain is abundant in synaptic genes and shows differences at the exon-intron boundary. *Nat. Struct. Mol. Biol.* **19**, 1037–1043 (2012).
12. Miller, C. A. et al. Cortical DNA methylation maintains remote memory. *Nat. Neurosci.* **13**, 664–666 (2010).
13. Vanyushin, B. F., Mazin, A. L., Vasilyev, V. K. & Belozersky, A. N. The content of 5-methylcytosine in animal DNA: the species and tissue specificity. *Biochim. Biophys. Acta* **299**, 397–403 (1973).
14. Iyer, L. M., Zhang, D. & Aravind, L. Adenine methylation in eukaryotes: apprehending the complex evolutionary history and functional potential of an epigenetic modification. *Bioessays* **38**, 27–40 (2016).
15. Hattman, S., Kenny, C., Berger, L. & Pratt, K. Comparative study of DNA methylation in three unicellular eucaryotes. *J. Bacteriol.* **135**, 1156–1157 (1978).
16. Hattman, S. DNA-[adenine] methylation in lower eukaryotes. *Biochemistry* **70**, 550–558 (2005).
17. Fu, Y. et al. N6-methyldeoxyadenosine marks active transcription start sites in *Chlamydomonas*. *Cell* **161**, 879–892 (2015).
18. Zhang, G. et al. N6-methyladenine DNA modification in Drosophila. *Cell* **161**, 893–906 (2015).
19. Ma, C. et al. N6-methyldeoxyadenine is a transgenerational epigenetic signal for mitochondrial stress adaptation. *Nat. Cell Biol.* https://doi.org/10.1038/s41556-018-0238-5 (2018).
20. Yao, B. et al. DNA N6-methyladenine is dynamically regulated in the mouse brain following environmental stress. *Nat. Commun.* **8**, 1122 (2017).
21. Usheva, A. & Shenk, T. TATA-binding protein-independent initiation: YY1, TFIIB, and RNA polymerase II direct basal transcription on supercoiled template DNA. *Cell* **76**, 1115–1121 (1994).
22. Bredy, T. W. et al. Histone modifications around individual BDNF gene promoters in prefrontal cortex are associated with extinction of conditioned fear. *Learn. Mem.* **14**, 268–276 (2007).
23. Liu, J. et al. Abundant DNA 6 mA methylation during early embryogenesis of zebrafish and pig. *Nat. Commun.* **7**, 13052 (2016).
24. Wu, T. P. et al. DNA methylation on N(6)-adenine in mammalian embryonic stem cells. *Nature* **532**, 329–333 (2016).
25. Ataman, B. et al. Evolution of Osteocrin as an activity-regulated factor in the primate brain. *Nature* **539**, 242–247 (2016).

26. Xiao, C.-L. et al. N^6-Methyladenine DNA Modification in the Human Genome. *Mol. Cell* **71**, 306–318.e7 (2018).
27. Xie, Q. et al. N^6-methyladenine DNA Modification in Glioblastoma. *Cell* **175**, 1228–1243.e20 (2018).
28. Luo, G.-Z. et al. Characterization of eukaryotic DNA N(6)-methyladenine by a highly sensitive restriction enzyme-assisted sequencing. *Nat. Commun.* **7**, 11301 (2016).
29. Vovis, G. F. & Lacks, S. Complementary action of restriction enzymes endo R-DpnI and Endo R-DpnII on bacteriophage f1 DNA. *J. Mol. Biol.* **115**, 525–538 (1977).
30. Lacks, S. & Greenberg, B. A deoxyribonuclease of *Diplococcus pneumoniae* specific for methylated DNA. *J. Biol. Chem.* **250**, 4060–4066 (1975).
31. Birnboim, H. C., Sederoff, R. R. & Paterson, M. C. Distribution of polypyrimidine. Polypurine segments in DNA from diverse organisms. *Eur. J. Biochem.* **98**, 301–307 (1979).
32. Manor, H., Rao, B. S. & Martin, R. G. Abundance and degree of dispersion of genomic d(GA)n.d(TC)n sequences. *J. Mol. Evol.* **27**, 96–101 (1988).
33. Soeller, W. C., Poole, S. J. & Kornberg, T. In vitro transcription of the *Drosophila* engrailed gene. *Genes Dev.* **2**, 68–81 (1988).
34. Biggin, M. D. & Tjian, R. Transcription factors that activate the Ultrabithorax promoter in developmentally staged extracts. *Cell* **53**, 699–711 (1988).
35. Wallrath, L. L. & Elgin, S. C. Position effect variegation in Drosophila is associated with an altered chromatin structure. *Genes Dev.* **9**, 1263–1277 (1995).
36. Stephens, C., Reisenauer, A., Wright, R. & Shapiro, L. A cell cycle-regulated bacterial DNA methyltransferase is essential for viability. *Proc. Natl Acad. Sci. USA* **93**, 1210–1214 (1996).
37. Liu, P. et al. Deficiency in a glutamine-specific methyltransferase for release factor causes mouse embryonic lethality. *Mol. Cell. Biol.* **30**, 4245–4253 (2010).
38. Ghosh, A., Carnahan, J. & Greenberg, M. E. Requirement for BDNF in activity-dependent survival of cortical neurons. *Science* **263**, 1618–1623 (1994).
39. Peters, J., Kalivas, P. W. & Quirk, G. J. Extinction circuits for fear and addiction overlap in prefrontal cortex. *Learn. Mem.* **16**, 279–288 (2009).
40. Lubin, F. D., Roth, T. L. & Sweatt, J. D. Epigenetic regulation of BDNF gene transcription in the consolidation of fear memory. *J. Neurosci.* **28**, 10576–10586 (2008).
41. West, A. E. Biological functions of activity-dependent transcription revealed. *Neuron* **60**, 523–525 (2008).
42. Sakata, K. et al. Role of activity-dependent BDNF expression in hippocampal-prefrontal cortical regulation of behavioral perseverance. *Proc. Natl Acad. Sci. USA* **110**, 15103–15108 (2013).
43. Simon, J. M., Giresi, P. G., Davis, I. J. & Lieb, J. D. Using formaldehyde-assisted isolation of regulatory elements (FAIRE) to isolate active regulatory DNA. *Nat. Protoc.* **7**, 256–267 (2012).
44. Ratel, D., Ravanat, J.-L., Berger, F. & Wion, D. N6-methyladenine: the other methylated base of DNA. *Bioessays* **28**, 309–315 (2006).
45. Low, D. A., Weyand, N. J. & Mahan, M. J. Roles of DNA adenine methylation in regulating bacterial gene expression and virulence. *Infect. Immun.* **69**, 7197–7204 (2001).
46. Wang, Y., Chen, X., Sheng, Y., Liu, Y. & Gao, S. N6-adenine DNA methylation is associated with the linker DNA of H2A.Z-containing well-positioned nucleosomes in Pol II-transcribed genes in Tetrahymena. *Nucleic Acids Res.* **45**, 11594–11606 (2017).
47. Kigar, S. L. et al. N^6-methyladenine is an epigenetic marker of mammalian early life stress. *Sci. Rep.* **7**, 18078 (2017).
48. Li, X., Baker-Andresen, D., Zhao, Q., Marshall, V. & Bredy, T. W. Methyl CpG binding domain ultra-sequencing: a novel method for identifying inter-individual and cell-type-specific variation in DNA methylation. *Genes Brain Behav.* **13**, 721–731 (2014).

Acknowledgements

The authors gratefully acknowledge grant support from the NIH (no. 5R01MH105398 to T.W.B. and P.B.; no. 5R01MH109588 to R.C.S. and T.W.B., no. 1R01GM123558 to P.B., no.1DP2GM119164 to R.C.S.; R.C.S. receives support from a Pew Scholar award), the NHMRC (nos. GNT1033127 and GNT1160823 to T.W.B.), the Conselho Nacional de Desenvolvimento Científico e Tecnológico (no. CNPq-CsF-400850/2014-1 to R.G.-O.), the Coordenação de Aperfeiçoamento de Pessoal de Nivel Superior – Brasil (CAPES-Finance Code 001 to R.G.O.) and the Research Council of Norway (FRIMEDBIO grant 32222 to M.B.). X.L. has been supported by postgraduate scholarships from the University of Queensland and the ANZ Trustees Queensland, The University of Queensland developmental fellowship and the ARC Discovery Early Career Researcher Award (no. DE190101078). PROMEC is funded by the Faculty of Medicine and Health Sciences at NTNU and the Central Norway Regional Health Authority. The authors also thank R. Tweedale for helpful editing of the manuscript and S. Gandhi for comments and lively discussion.

Author contributions

X.L. prepared lentiviral constructs carried out the experiments and wrote the manuscript. Q.Z. performed all the bioinformatics analysis and wrote the manuscript. W.W. prepared lentiviral constructs, carried out the chIP assay and qPCR experiments and performed FACS sorting of activated neurons in RNA-seq experiment. Q.L. built the N6amt1 overexpression constructs. C.M. performed bioinformatics analysis. M.R.E., L.E.W. and T.W.B. performed behavioral experiments. P.R.M. prepared the immunohistochemistry. J.Y. performed protein analysis on the in vivo experiments. S.U.M. performed behavioral experiments. Z.W. performed the western blot on N6amt1 overexpression in HEK cells. S.N. performed RNA and DNA extraction. C.B.V. performed mass spectrometry experiments. E.L.Z. performed quantitaitive PCR experiments. K.K. performed protein studies. R.G.-O. contributed reagents and helped write the manuscript. M.B. contributed reagents and helped write the manuscript. P.F.B. contributed access to the bioinformatic analysis pipeline and helped write the manuscript. R.C.S. contributed reagents and helped write the manuscript. T.W.B. conceived the study, designed experiments and wrote the manuscript.

Competing interests

The authors declare no competing interests.

Additional information

Supplementary information is available for this paper at https://doi.org/10.1038/s41593-019-0339-x.

Reprints and permissions information is available at www.nature.com/reprints.

Correspondence and requests for materials should be addressed to X.L. or T.W.B.

Journal peer review information Nature Neuroscience thanks Ian Maze and other anonymous reviewer(s) for their contribution to the peer review of this work.

Publisher's note: Springer Nature remains neutral with regard to jurisdictional claims in published maps and institutional affiliations.

Methods

Mice. Male C57BL/6 mice (10–14 weeks old) were housed four per cage, maintained on a 12 h light/dark time schedule and allowed free access to food and water. All testing took place during the light phase in red-light-illuminated testing rooms following protocols approved by the Institutional Animal Care and Use Committee of the University of California, Irvine and by the Animal Ethics Committee of The University of Queensland. Animal experiments were carried out in accordance with the Australian Code for the Care and Use of Animals for Scientific Purposes (8th edition, revised 2013).

DNA/RNA extraction. Tissue derived from the ILPFC of retention control or EXT trained mice was homogenized by a Dounce tissue grinder in 500 µl of cold 1 PBS (Gibco). Then 400 µl of homogenate was used for DNA extraction and 100 µl was used for RNA extraction. DNA extraction was carried out using a DNeasy Blood & Tissue Kit (Qiagen) with RNAse A (5 prime), RNAse H and RNAse T1 treatment (Invitrogen) and RNA was extracted using Trizol reagent (Invitrogen). Both extraction protocols were conducted according to the manufacturer's instructions. The concentrations of DNA and RNA were measured by Qubit assay (Invitrogen).

LC–MS/MS. Genomic DNA was enzymatically hydrolyzed to deoxynucleosides by the addition of benzonase (25 U, Santa Cruz Biotech), nuclease P1 (0.1 U, Sigma-Aldrich) and alkaline phosphatase from *E. coli* (0.1 U, Sigma-Aldrich) in 10 mM ammonium acetate pH 6.0, 1 mM $MgCl_2$ and 0.1 mM erythro-9-(2-hydroxy-3-nonyl) adenine. After 40 min incubation at 40 °C, three volumes of acetonitrile were added to the samples and centrifuged (16,000*g*, 30 min, 4 °C). The supernatants were dried and dissolved in 50 µl of 5% methanol in water (v/v) for LC–MS/MS analysis of modified and unmodified nucleosides. Chromatographic separation was performed on a Shimadzu Prominence high-performance liquid chromatography system for m6dA, and by means of an Ascentis Express F5 150 × 2.1 mm^2 internal diameter (2.7 µm) column equipped with an Ascentis Express F5 12.5 × 2.1 mm^2 internal diameter (2.7 µm) guard column (Sigma-Aldrich) for unmodified deoxynucleosides. The mobile phase consisted of water and methanol (both containing 0.1% formic acid) for m6dA, starting with a 4-min gradient of 5–50% methanol, followed by 6 min re-equilibration with 5% methanol, and for unmodified deoxynucleosides maintaining isocratically with 30% methanol. The mobile phase consisted of 5 mM acetic acid and methanol, starting with a 3.5-min gradient of 5–70% methanol, followed by 4 min re-equilibration with 5% methanol. Mass spectrometry detection was performed using an API5500 triple quadrupole (AB Sciex) operating in positive electrospray ionization mode for m6dA and unmodified deoxynucleosides, or negative mode for m6dA. The LC-MS/MS analysis was perfromed by the Proteomics and Modomics Experimental Core Facility (PROMEC), Norwegian University of Science and Technology (NTNU).

Dot blot. Total DNA was diluted with 0.1 N NaOH (Sigma) to 2 µl and spotted on to a nitrocellulose membrane (BioRad). This was followed by 10 min incubation at room temperature. DNA was hybridized to the membrane with 15 min incubation at 80 °C. The membrane was blocked in blocking buffer (LI-COR) for 60 min. The membrane was then incubated with a 1:1,000 dilution of m6A (Active Motif) at 4 °C overnight. After three rounds of washes with 1× Tris buffered saline-Tween (TBS-T), the membrane was incubated with 1:15,000 goat anti-rabbit secondary antibody conjugated with AlexaFluor 680 (LI-COR). The membranes were then washed with 1× TBS-T and imaged, and the intensity score of each dot was analyzed by the Odyssey Fc system and normalized to the background.

qRT–PCR. 1 µg of total RNA was used for complementary DNA synthesis using the PrimeScript Reverse Transcription Kit (Takara). Quantitative PCR was carried out on a RotorGeneQ (Qiagen) cycler with SYBR Green Master Mix (Qiagen) using primers for target genes and for beta-actin as an internal control (Supplementary Table 1). All transcript levels were normalized to beta-actin mRNA using the ΔΔCT method and each PCR reaction was run in duplicate for each sample and repeated at least twice.

DNA shearing. DNA and chromatin were sheared using the m220 Ultra-sonicator (Covaris) with an average size of roughly 300 bp. The program was set as follows: peak power, 50; duty factor, 20; cycle/burst, 200; duration, 75 s and temperature in the range of 18–22 °C for DNA shearing and 7–10 °C for chromatin shearing.

ChIP. ChIP was performed following modification of the Invitrogen ChIP kit protocol. Tissue was fixed in 1% formaldehyde and cross-linked cell lysates were sheared by Covaris in 1% SDS lysis buffer to generate chromatin fragments with an average length of 300 bp by using peak power, 75; duty factor, 2; cycle/burst, 200; duration, 900 s and temperature between 5 and 9 °C. The chromatin was then immunoprecipitated using previously validated antibodies for H3K4me[49], YY1 (ref. [50]), TFIIB[51] and RNA Pol II (ref. [52]). An equivalent amount of normal rabbit IgG (Cell Signaling) or mouse IgG (Santa Cruz) was also used for non-specificity control. Antibody and sample mixtures were then incubated overnight at 4 °C. Protein–DNA–antibody complexes were precipitated with protein G-magnetic beads (Invitrogen) for 1 h at 4 °C, followed by three washes in low salt buffer and three washes in high salt buffer. The precipitated protein–DNA complexes were eluted from the antibody with 1% SDS and 0.1 M $NaHCO_3$, then incubated 4 h at 60 °C in 200 mM NaCl to reverse the formaldehyde cross-link. Following proteinase K digestion, phenol-chloroform extraction and ethanol precipitation, samples were subjected to qPCR using primers specific for 200-bp segments corresponding to the target regions. Samples that did not reach data from IgG enrichment were excluded. Detailed antibody information is included in the Reporting Summary file.

DpnI-seq. Frozen ILPFC tissues were homogenized and fixed with 1% methanol free PFA (Thermo Fisher) at room temperature for 5 min. A final concentration of 0.125 mM of glycine was then added to stop fixation. The cells were washed with 1× cold PBS three times and the cell suspension treated with DNase I (Thermo Fisher) for 15 min at 4 °C followed by 1 ml of 1× cold PBS wash. The cell suspension was blocked by using FACS blocking buffer (1× BSA, 1× normal goat serum and 1% Triton-X) for 15 min at 4 °C with end-to-end rotation. After 15 min, the cell suspension was incubated with a 1:150 dilution of preconjugated Arc antibody (Bioss) and a 1:300 dilution of preconjugated NeuN antibody (Bioss) at 4 °C for 1 h with an end-to-end rotation. Following incubation, two rounds of 1 ml 1× cold PBS washes were applied. Then the cell pellets were resuspended with 500 µl of 1× cold PBS and 1:2,000 DAPI was added. FACS was performed on a BD FACSAriaII (BD Science). DNA was extracted from FACS-sorted cells using phenol-chloroform. 10 ng of genomic DNA was used for DpnI-seq, sequence library preparation was prepared following a previously published protocol[28] and samples were sequenced on a HiSeq4000 at University of California Irvine's genomic sequencing facility with 150-bp paired-end reads.

FACS-sorted RNA-seq. Tissue was dissociated with FACS lysis buffer (final concentration: 0.32 M sucrose, 10 mM Tris-HCl pH 8.0, 5 mM $CaCl_2$, 3 mM $Mg(acetate)_2$, 0.1 mM EDTA, 1 mM DTT, 0.3% Triton-X100 and 100× PIC) into a single-cell suspension, then fixed with 1% formaldehyde for 5 min and stopped by 0.125 M Glycine. Cells were washed twice with cold 1× PBS to remove excess formaldehyde and glycine. After incubating with blocking buffer (final concentration: 10% normal goat serum, 5% BSA, 0.1% Triton-X100 and 1× PIC) for 30 min, cells were double-labeled with Arc antibody (Bioss) in 1:20,000 dilution per million cells and NeuN antibody (Abcam) in 1:20,000 per million cells, together with DAPI (Thermo Fisher) in 1:2,000. PBPT buffer was used for washing (twice each time) and resuspended in 500 µl 1× PBS for FACS sorting. FACS was performed on a BD FACSArial (BD Science) and cells were sorted into a lysis buffer using the Arcturus PicoPure RNA isolation kit (Applied Biosystems). RNA was isolated from sorted cells using the Arcturus PicoPure RNA isolation kit (Applied Biosystems) following the manufacturer's protocol. Then, 5 ng of total RNA per sample and the SMRTer Stranded Total RNA-seq Kit v.2 Pico Input Mammalian Components kit (Clontech) were used for RNA-seq library preparation following the manufacturer's protocol. Sequencing was conducted at GENEWIZ (Suzhou, China) with 150bp paired-end reads.

N6amt1 ChIP-seq. N6amt1 ChIP was performed as previously described. After ChIP (using 4 µg of the antibody), DNA was extracted using the DNA Clean and Concentrator kit (Zymo Research). Then, 10 ng of enriched DNA per sample and KAPA DNA HyperPrep kit (Roche) was used for ChIP-seq library preparation following the manufacturer's protocol. The sequencing run was performed on the Illumina Nextseq platform at the University of Queensland's genome sequencing facility.

DpnI-seq data analysis. Illumina pair-end sequencing data was aligned to the mouse reference genome (mm10) using BWA (v.0.6.2)[53]. Samtools (v.0.1.17)[54] was then used to convert 'SAM' files to 'BAM' files, sort and index the BAM files and remove any duplicate reads. Reads with low mapping quality (<20) or reads that were not properly paired-end aligned to the reference genome were excluded from the downstream analysis. These steps ensured that only high-quality alignments were used for the analysis of DpnI cleavage sites (Supplementary Table 2). After alignment, we applied a similar approach that inferred potential DpnI cleavage sites based on the position of 5' ends as described in a previous study[28]. Briefly, a binominal distribution model was assumed that each read could be randomly sheared and aligned to the genome with a probability $P = 1/gs$ (where gs is genome size) or cleaved by DpnI. For each individual sample, let n be the total number of reads. The P value of each genomic locus supported by x number of reads was calculated as $C_n^x p^x (1-p)^{n-x}$. The Bonferroni correction was then applied for a multiple testing correction. A genomic locus was determined as a real DpnI cleavage site if it satisfied the following criteria: (1) the corrected P value was <0.01 in at least two of the three biological replicates in one or both conditions and (2) the locus was not in the mm10 empirical blacklists identified by the ENCODE consortium[55].

The detected DpnI cleavage sites in each condition as well as merged data were used for motif analysis separately. A DpnI cleavaged 'GATC' site was determined as a differentially methylated site between retention control and EXT conditions if it satisfied the following criteria: (1) the DpnI cleavage site was supported by at least two biological replicates in one condition (for example, condition A) but at most by one replicate in the other condition (for example, condition B); (2) all three

biological replicates in condition A had 5' end(s) supporting the DpnI site and (3) the number of 5' end supported reads in condition A was at least twofold more than in condition B. Genes with differentially methylated GATC sites near the TSS region (±500 bp) were parsed for gene ontology enrichment analysis using DAVID (v.6.8)[56,57].

N6amt1 ChIP-seq data analysis. We performed the paired-end read alignment and filter using the same analysis workflow as described for DpnI-seq data analysis. After removing the duplicate reads, low mapping quality reads and paired-end reads that were not properly aligned, MACS2 (v.2.1.1.20160309) was used to call peaks for each sample using the parameter setting 'callpeak -t SAMPLE -c INPUT -f BAMPE–keep-dup = all -g mm -p 0.05 -B'. Peak summits identified by MACS2 from all samples were collected to generate a list of potential binding sites. Custom PERL script was then applied to parse the number of fragments (hereafter referred to as counts) that covered the peak summit in each sample. Each pair of properly paired-end aligned reads covering the peak summit represented one count. The total counts in each sample were normalized to 20 million before comparison among samples. The potential binding sites were kept if they met all of the following conditions: (1) the sites were not located in the mm10 empirical blacklists and (2) the normalized counts in all three biological replicates in one group were larger than in its input sample, and the normalized counts in at least two replicates were more than twofold larger than in the normalized input count.

RNA-seq data analysis. Illumina paired-end reads were aligned to the mouse reference genome (mm10) using HISAT2 (v.2.0.5), with the parameter setting of '–no-unal–fr–known-splicesite-infile mm10_splicesites.txt'. The 'htseq-count' script in HTSeq package (v.0.7.1) (http://www-huber.embl.de/HTSeq) was used to quantify the gene expression level by generating a raw count table for each sample. On the basis of these raw count tables, edgeR (v.3.16.5) was adopted to perform the differential expression analysis between groups. EdgeR used a trimmed mean of *M* values to compute scale factors for library size normalization. Genes with counts per million >1 in at least three samples were kept for downstream analysis. We applied the quantile-adjusted conditional maximum likelihood method to estimate dispersions and the quasi-likelihood *F*-test to determine differential expression. Differentially expressed genes between two groups were identified when false discovery rate was <0.05. Gene ontology enrichment analysis for differentially expressed genes was performed using the functional annotation tool in DAVID Bioinformatics Resources (v.6.8)[56,57].

Determine distance from m6dA sites to N6amt1 sites. For each N6amt1 binding site (peak summit) located in TSS ±500bp regions, we searched its nearby m6A sites and extracted the distance between the peak summit and its closest m6A site. The distribution plot (Fig. 4g) shows that most N6amt1 binding sites have a nearby m6A site within 500 bp and with the 0–200 bp range being the most abundant.

m6dA MeDIP–DIP. One microgram of genomic DNA was diluted to 130 µl ultrapure water (Invitrogen) and sheared with an average size about 300 bp before the capture. m6dA captured was performed using a m6dA antibody (Active Motif) to capture m6dA enriched genomic regions. The procedure was adapted from the manufacturer's protocol for methyl DNA immunoprecipitation (Active Motif). Then, 500 ng of sheared DNA and 4 µg of m6dA antibody were used for each immunoprecipitation reaction and all selected targets (GATC site proximal BDNF P4: Chr2: 109692436-109692774; distal GATC site: Chr2: 109691953-109692103) were normalized to input DNA and then to their own controls by using the ΔΔCT method. Each qPCR reaction was run in duplicate for each sample and repeated at least twice. Samples that did not reach data from IgG enrichment were excluded.

DpnI–qPCR. Three hundred nanograms of sheared DNA was treated with 200 units of DpnI (NEB) for 16 h at 37 °C and followed by heat inactivation using 80 °C for 20 min. Treated DNA was then used in qPCR reactions. All selected targets were normalized to their own untreated control by using the ΔΔCT method, and each PCR reaction was run in duplicate for each sample and repeated at least twice. A schema is included in Fig. 1b.

FAIRE–qPCR. The procedure was adapted from a previously published protocol[11]. ILPFC tissues were homogenized in 500 µl of PBS. Molecular grade formaldehyde (16%, Thermo Fisher) was added directly to the cell suspension at room temperature (22–25 °C) to a final concentration of 1% and incubated for 5 min. Glycine was then added to a final concentration of 125 mM for 5 min at room temperature to stop fixation. Two rounds of PBS wash were performed and the cells were collected by centrifugation at 2,000 r.p.m. for 4 min and stored at −80 °C. Fixed cell pellets were then treated with ChIP lysis buffer as described above and samples sonicated using Covaris to generate chromatin fragments with an average length of 300 bp (using peak power, 75; duty factor, 2; cycle/burst, 200; duration, 900 s and a temperature between 5 and 9 °C). Cellular debris was cleared by centrifugation at 15,000 r.p.m. for 10 min at 4 °C. DNA was isolated by adding an equal volume of phenol-chloroform (Sigma), and followed by vortex and centrifugation at 15,000 r.p.m. for 15 min at 4 °C. The aqueous phase was isolated and stored in a fresh 1.5 ml microcentrifuge tube. An additional 500 µl of TE buffer was added to the organic phase, vortexed and centrifuged again at 15,000 r.p.m. for 15 min at 4 °C. The aqueous phase was isolated and combined with the first aqueous fraction. Another phenol-chloroform extraction was performed on the pooled aqueous fractions to ensure that all protein was removed. The DNA was isolated by the previously described DNA extraction procedures in the ChIP protocol. Input DNA isolation was carried out as previously described. qPCR was carried out using SYBR Green Master Mix (Qiagen) on a Rotorgene platform (Qiagen). Relative enrichment of each target in the FAIRE-treated DNA was calculated on the basis of untreated input DNA.

N6amt1 knockdown constructs. Lentiviral plasmids were generated by inserting N6amt1, N6amt2 shRNA or scrambled control fragments (Supplementary Table 1) immediately downstream of the human H1 promoter in a modified FG12 vector (FG12H1, derived from the FG12 vector originally provided by D. Baltimore, CalTech) as previously described[2]. Lentivirus was prepared and maintained according to protocols approved by the Institutional Biosafety Committee at the University of California, Irvine and the University of Queensland.

N6amt1 overexpression lentiviral constructs. Lentiviral plasmids were generated by inserting a full mouse N6amt1 transcript cDNA with green fluorescent protein (GFP) from a FUGW (Addgene) backbone. First, a full length of n6amt1 cDNA was PCR amplified from N6amt1 (Myc-DDK-tagged) construct (Origene cDNA clone no. MR227618). The forward primer was 5'-ATTCGTCGACTGGATCCGGT. The reverse primer was 5'-CCGAATTCGGCCGG CCGTTTAAACCTT. The PCR amplified fragments were inserted immediately downstream of the Ubiquitin C promoter of a lentiviral vector, FUIGW-K1. The original FUGW vector was used as an Empty vector control. Either N6amt1 overexpression or the control plasmid was co-transfected with lentiviral helper plasmids (pMDL, pVSVG and pREV) into HEK 293 T cells with roughly 80% confluence. Then 4 h later, sodium butyrate was added to stimulate viral production. After 2 days' incubation at 37 °C and 5% CO_2, the virus was collected by ultracentrifugation. The titer was measured with Lenti-X Gostix (Clontech).

Titration of virus. A six-well plate with 4×10^5 293 T cells per well was prepared the day before titration of the virus. The next day, the number of cells in each well were estimated by counting. Then, each virus was added at amounts of 0.5, 1, 2 and 5 µl per well and incubated for 2–3 days. The percentage of cells expressing enhanced GFP was used to calculate the virus titer by using the following formula: %GFP positive cells (e.g., 20% = 0.2) × 1 µl of virus added to well × number of cells in well before infection (e.g., 1×10^6) = infectious units (IU)/ml × 10^3 = titration of virus. Only viruses that reached over 1×10^8 IU/ml were used in this study.

Cannulation surgery and lentiviral infusion. A double cannula (PlasticsOne) was implanted in the anterior–posterior plane, ±30° along the midline and into the ILPFC a minimum of 3 days before viral infusion. The coordinates of the injection locations were centered at +1.80 mm in the anterior–posterior plane and −2.7 mm in the dorsal-ventral plane. For PLPFC cannulation surgery, the coordinates of the injection locations were centered at +1.80 mm in the anterior–posterior plane, −2.0 mm in the dorsal-ventral plane and 0 mm in the medial-lateral plane. Then 1.0 µl of lentivirus was introduced bilaterally via two injections delivered within 48 h. For knockdown experiments, mice were first fear conditioned, followed by two lentiviral infusions 24 h post fear condition training and, after a 1-week incubation period, they were then extinction trained. After training, viral spread was verified by immunohistochemistry according to a previously published protocol[2].

Lentiviral knockdown and overexpression (OX) of N6amt1, in vitro. One microgram of N6amt1 shRNA/OX or scrambled control/empty vector control lentivirus was applied to primary cortical neurons in a six-well plate. After 7 days' incubation, cells were gathered for RNA extraction.

Behavioral tests. Two contexts (A and B) were used for all behavioral fear testing. Both conditioning chambers (Coulbourn Instruments) had two transparent walls and two stainless steel walls with a steel grid floors (3.2 mm in diameter, 8 mm centers); however, the grid floors in context B were covered by a flat white plastic non-transparent surface with two white light emitting diodes to minimize context generalization. Individual digital cameras were mounted in the ceilings of each chamber and connected via a quad processor for automated scoring by a freezing measurement program (FreezeFrame). Fear conditioning was performed in context A with spray of vinegar (10% distilled vinegar). Then, the actual fear condition protocol was started with 120 s pre-fear conditioning incubation, followed by three pairings of a 120 s, 80 dB, 16 kHz pure tone conditioned stimulus co-terminating with a 1 s (at 2 min intervals) 0.7 mA foot shock (unconditioned stimulus). Mice were randomly counterbalanced into equivalent treatment groups on the basis of freezing during the third training conditioned stimulus. Animals that did not reach 30% freezing behavior during the last conditioned stimulus were excluded. For extinction, mice were exposed in context B with a stimulus light on and spray of almond (10% almond extract and 10% ethanol). Mice were acclimatized for 2 min,

then extinction training comprised 60 non-reinforced 120 s conditioned stimulus presentations (at 5-s intervals). For behavior control experiments, context exposure was performed for both the fear condition and fear extinction training. These animals were only exposed to either context A or B for equal amounts of time to the mice in the fear or fear extinction conditions, but were not exposed to any three conditioned stimulus-unconditioned stimulus or 60 conditioned stimulus. For the retention test, all mice were returned to context B and following a 2 min acclimatization (used to minimize context generalization), freezing was assessed during three 120 s conditioned stimulus presentations (with 120 s intertribal interval). Animals were randomly selected for extinction memory test and freezing scores were automatically assessed using FreezeFrame (Colbourn). Memory was calculated as the percentage of time spent freezing during the tests. Animals that showed a off target injection or not effective gene knockdown were exlcluded from the study.

Behavioral training (for tissue collection). Naïve animals remained in their home cage until euthanasia. For the other groups, fear conditioning consisted of three pairings (120 s inner-trial interval, ITI) of a 120 s, 80 dB, 16 kHz pure tone conditioned stimulus co-terminating with a 1 s, 0.7 mA foot shock in context A. Mice were matched into equivalent treatment groups on the basis of freezing behavior during the third training conditioned stimulus. The context A exposure group spent an equivalent amount of time in context A without any conditioned and unconditioned stimulus. One day later, the fear-conditioned mice were brought to context B, where the EXT group was presented with 60 conditioned stimulus presentations (5 s ITI). The fear-conditioned without extinction (FC No EXT) group spent an equivalent amount of time in context B without any conditioned stimulus presentations. Animals that showed a significant reduction in fear were excluded. For pseudoconditioned controls (PseudoCon + EXT) group, mice were exposed to three unpaired tones and foot shocks in context A on day 1. These mice then underwent the normal 60 conditioned stimuli for extinction training the day in context B. Tissue was collected from these groups immediately after the end of either context B exposure (FC No EXT) or extinction training (EXT).

Primary cortical neuron, N2A and HEK cell culture. Cortical tissue was isolated from E15 mouse embryos in a sterile atmosphere. Tissue was dissociated by finely chopping, followed by gentle pipetting to create a single-cell suspension. To prevent clumping of cells due to DNA from dead cells, tissue was treated with 2 units per µl of DNase I. Cells finally went through the 40 µm cell strainer (BD Falcon) and were plated onto a six-well plate coated with poly-L-ornithine (Sigma P2533) at a density of 1×10^6 cells per well. The medium used was Neurobasal media (Gibco) containing a B27 supplement (Gibco), 1× GlutaMAX (Gibco) and 1% Pen/Strep (Sigma). The N2a cell was maintained in a medium containing half DMEM and high glucose (Gibco), and half OptiMEM 1 (Gibco) with 5% serum and 1% Pen/Strep. The HEK293t cell was maintained in a medium containing DMEM and high glucose (Gibco) with 5% serum and 1% Pen/Strep (Gibco).

Western blot. Protein samples were extracted by using NP40 solution following the manufacturer's protocol (Thermo Fisher) and protein concentration was determined by using the Qubit protein detection kit (Invitrogen), also following the manufacturer's protocol. Individual samples were run on a single 10-well gel or 12-well pre-made 4–12% gel (Thermo Fisher). Briefly, samples were prepared on ice (to a final volume of 20 µl) and then vortexed and denatured for 10 min at 90 °C. Gels were run with 1× TBS-T and proteins were transferred onto a nitrocellulose membrane (Biorad). The membrane was blocked by blocking buffer (LI-COR) for 1 h at room temperature, washed with TBS-T for 5 min (three times) and incubated with 5 ml of N6amt1 (1:250; Santa Cruz) and Beta-actin (1:500; Santa Cruz) or beta-tubulin (1:500; Santa Cruz) antibodies in blocking buffer (LI-COR) overnight at 4 °C. The membranes were washed with TBS-T (three times), incubated for 1 h with anti-mouse secondary antibody (1:15,000; LI-COR) and anti-rabbit secondary antibody (1:15,000; LI-COR) in blocking buffer (LI-COR), then washed three times with TBS-T for 10 min (five times) and 20 min (once). Absorbance readings of the membrane were taken using a LI-COR FX system following the manufacturer's protocol. Detailed antibody information is included in the Reporting Summary file.

Statistical analyses. No statistical methods were used to pre-determine sample sizes but our sample sizes are similar to those reported in previous publications[2,22]. In all cases where an unpaired *t*-test was used, we opted for a one-tailed test with an a priori hypothesis that the accumulation of m6dA is permissive for gene expression and memory formation. Therefore, all experiments related to epigenetic and transcriptional machinery were proposed to show a positive correlation with m6dA, hence, a one-tailed test was used. For behavioral analysis, freezing (the absence of all non-respiratory movement) was rated during all phases by an automated digital analysis system using a 5-s instantaneous time sampling technique. The percentage of observations with freezing was calculated for each mouse and data represent the mean ± s.e.m. freezing percentages for groups of mice during specified time bins. Total session means were analyzed using a one-way ANOVA for the behavioral data in Fig. 6 and Supplementary Fig. 11. In experiments using viral manipulation and Bdnf rescue, all data analysis was carried out using two-way ANOVA for the data in Figs. 6 and 7 and Supplementary Fig. 11. Dunnett's posthoc tests were used where appropriate. For DpnI–qPCR on FACS sorted samples in Supplementary Fig. 3, two-way ANOVA was used followed by Dunnett's posthoc tests. For behavioral studies, there was no blinding to group allocation since the groups were counterbalanced on the basis of fear conditioning. During behavioral tests, the data were captured and analyzed using a fully automatic analysis program. For immunohistochemistry, FACS and sequencing, the investigators were blind to group allocation during data collection and analysis.

Reporting Summary. Further information on research design is available in the Nature Research Reporting Summary linked to this article.

Data availability

All sequencing raw fastq files have been deposited at the Sequence Read Archive (accession SRP110529) and BioProject (accession PRJNA391201). All customized code is free and accessible at Github for download at https://github.com/Qiongyi/2018_DPNI-Seq_study.

References

49. Jung, M. et al. Longitudinal epigenetic and gene expression profiles analyzed by three-component analysis reveal down-regulation of genes involved in protein translation in human aging. *Nucleic Acids Res.* **43**, e100 (2015).
50. Song, G. & Wang, L. Nuclear receptor SHP activates miR-206 expression via a cascade dual inhibitory mechanism. *PLoS One* **4**, e6880 (2009).
51. Pan, H. et al. Negative elongation factor controls energy homeostasis in cardiomyocytes. *Cell Rep.* **7**, 79–85 (2014).
52. Chaudhary, P. et al. HSP70 binding protein 1 (HspBP1) suppresses HIV-1 replication by inhibiting NF-κB mediated activation of viral gene expression. *Nucleic Acids Res.* **44**, 1613–1629 (2016).
53. Li, H. & Durbin, R. Fast and accurate short read alignment with Burrows–Wheeler transform. *Bioinformatics* **25**, 1754–1760 (2009).
54. Li, H. et al. The Sequence Alignment/Map format and SAMtools. *Bioinformatics* **25**, 2078–2079 (2009).
55. Dunham, I. et al. An integrated encyclopedia of DNA elements in the human genome. *Nature* **489**, 57–74 (2012). ENCODE Project Consortium.
56. Huang, W., Sherman, B. T. & Lempicki, R. A. Bioinformatics enrichment tools: paths toward the comprehensive functional analysis of large gene lists. *Nucleic Acids Res.* **37**, 1–13 (2009).
57. Huang, W., Sherman, B. T. & Lempicki, R. A. Systematic and integrative analysis of large gene lists using DAVID bioinformatics resources. *Nat. Protoc.* **4**, 44–57 (2009).

nature research

Corresponding author(s): Timothy Bredy; Xiang Li

Last updated by author(s): Dec 19, 2018

Reporting Summary

Nature Research wishes to improve the reproducibility of the work that we publish. This form provides structure for consistency and transparency in reporting. For further information on Nature Research policies, see Authors & Referees and the Editorial Policy Checklist.

Statistics

For all statistical analyses, confirm that the following items are present in the figure legend, table legend, main text, or Methods section.

n/a	Confirmed	
☐	☒	The exact sample size (*n*) for each experimental group/condition, given as a discrete number and unit of measurement
☐	☒	A statement on whether measurements were taken from distinct samples or whether the same sample was measured repeatedly
☐	☒	The statistical test(s) used AND whether they are one- or two-sided *Only common tests should be described solely by name; describe more complex techniques in the Methods section.*
☐	☒	A description of all covariates tested
☐	☒	A description of any assumptions or corrections, such as tests of normality and adjustment for multiple comparisons
☐	☒	A full description of the statistical parameters including central tendency (e.g. means) or other basic estimates (e.g. regression coefficient) AND variation (e.g. standard deviation) or associated estimates of uncertainty (e.g. confidence intervals)
☐	☒	For null hypothesis testing, the test statistic (e.g. *F*, *t*, *r*) with confidence intervals, effect sizes, degrees of freedom and *P* value noted *Give P values as exact values whenever suitable.*
☒	☐	For Bayesian analysis, information on the choice of priors and Markov chain Monte Carlo settings
☒	☐	For hierarchical and complex designs, identification of the appropriate level for tests and full reporting of outcomes
☒	☐	Estimates of effect sizes (e.g. Cohen's *d*, Pearson's *r*), indicating how they were calculated

Our web collection on statistics for biologists contains articles on many of the points above.

Software and code

Policy information about availability of computer code

Data collection

Mass spectrometry detection was performed using an API5500 triple quadrupole and Analyst software 1.7 version (AB Sciex); Dot blot and western blot data were collected by by the Odyssey Fc system and Image studio version 5.0 (Licor) ; Quantitative PCR was performed on a RotorGeneQ (Qiagen) cycler and RotorGene Q software version 2.3.1.49; DpnI-seq data is collected by Hiseq4000 (illumina) and local run manager software 2.0 version. N6amt1 chIP-seq and RNA-seq is collected by Hiseq2500 (illumina) and local run manager software 2.0 version; Animal behavioral data was collected by Freezeframe (Colbourn) software version 4.

Data analysis

DpnI-seq Data analysis: Illumina pair-end sequencing data was aligned to the mouse reference genome (mm10) using BWA (v0.6.2) 6. Samtools (v0.1.17) 7was then used to convert “SAM” files to “BAM” files, sort and index the “BAM” files, and remove duplicate reads. Reads with low mapping quality (<20) or reads that were not properly paired-end aligned to the reference genome were excluded from the downstream analysis. These steps ensure that only high-quality alignments were used for the analysis of DpnI cleavage sites (Suppl. Table 2). After alignment, we applied a similar approach that infers potential DpnI cleavage sites based on the position of 5’ends as described in a previous study 5. Briefly, a binominal distribution model was assumed that each read could be randomly sheared and aligned to the genome with a probability p = 1/gs (gs = genome size) or cleaved by DpnI. For each individual sample, let n be the total number of reads. The P value of each genomic locus supported by x number of reads was calculated as C_n^x p^x 〖(1-p)〗 ^(n-x). Bonferroni correction was then applied for multiple testing correction. A genomic locus was determined as a real DpnI cleavage site if it satisfies the following criteria: i) the corrected P value < 0.01 in at least 2 of the 3 biological replicates in one condition or both conditions, and ii) the locus is not in the mm10 empirical blacklists identified by the ENCODE consortium 8.
N6amt1 ChIP-Seq data analysis: We performed the paired-end reads alignment and filter using the same analysis workflow as described in DpnI-Seq data analysis. After removed duplicate reads, low mapping quality reads, and not properly paired-end aligned reads, MACS2 (version 2.1.1.20160309) was used to call peaks for each sample with the parameter setting “callpeak -t SAMPLE -c INPUT -f BAMPE --keep-dup=all -g mm -p 0.05 -B”. Peak summits identified by MACS2 from all samples were collected to generate a list of potential binding sites. Custom PERL script was then applied to parse the number of fragments (hereafter referred as counts) that cover the peak summit in each sample. Each pair of properly paired-end aligned reads covering the peak summit represents one count. The total counts in each sample were normalised to 20 million before comparison among samples. The potential binding sites were kept if they met all of the following conditions: i) the sites were not located in the mm10 empirical blacklists, and ii) the normalized counts in all three biological

replicates in one group were larger than that in its input sample, and the normalized counts in at least 2 replicates were more than 2-folds larger than its normalized input count.
RNA-Seq data analysis: Illumina paired-end reads were aligned to the mouse reference genome (mm10) using HISAT2 (version 2.0.5), with the parameter setting of "--no-unal --fr --known-splicesite-infile mm10_splicesites.txt". The "htseq-count" script in HTSeq package (v0.7.1) (http://www-huber.embl.de/HTSeq) was used to quantitate the gene expression level by generating a raw count table for each sample. Based on these raw count tables, edgeR (version 3.16.5) was adopted to perform the differential expression analysis between groups. EdgeR used a trimmed mean of M-values to compute scale factors for library size normalization. Genes with counts per million (CPM) > 1 in at least 3 samples were kept for downstream analysis. We applied the quantile-adjusted conditional maximum likelihood (qCML) method to estimate dispersions and the quasi-likelihood F-test to determine differential expression. Differentially expressed genes between two groups were identified when FDR < 0.05. Gene ontology enrichment analysis for differentially expressed genes was performed using the functional annotation tool in DAVID Bioinformatics Resources (version 6.8).
Other data analysis that are include in this study were used Prim 7 (GraphPad)

For manuscripts utilizing custom algorithms or software that are central to the research but not yet described in published literature, software must be made available to editors/reviewers. We strongly encourage code deposition in a community repository (e.g. GitHub). See the Nature Research guidelines for submitting code & software for further information.

Data

Policy information about availability of data

All manuscripts must include a data availability statement. This statement should provide the following information, where applicable:

- Accession codes, unique identifiers, or web links for publicly available datasets
- A list of figures that have associated raw data
- A description of any restrictions on data availability

The raw data that support the findings of this study are available from the corresponding author upon reasonable request.

Field-specific reporting

Please select the one below that is the best fit for your research. If you are not sure, read the appropriate sections before making your selection.

☒ Life sciences ☐ Behavioural & social sciences ☐ Ecological, evolutionary & environmental sciences

For a reference copy of the document with all sections, see nature.com/documents/nr-reporting-summary-flat.pdf

Life sciences study design

All studies must disclose on these points even when the disclosure is negative.

Sample size	From many previous experiments, we know that groups of 8 animals are sufficient to obtain statistically reliable results under the conditions of our experiments and typical effect sizes. This was calculated from the average of 13 experiments where the average freezing score during the last CS of a standard 3 CS-US fear conditioning protocol was 62.12% and the average freezing score on a subsequent behavioural task was 48.04%. Assuming a common standard deviation of 10, and performing a 2-sided test with alpha .05 and power of .80, we can obtain sufficient statistical power from 8 animals. In some cases, we present results from n=7 due to the loss of animals from the experiment prior to data collection
Data exclusions	There are data points excluded from the ChIP experiment because the binding efficiency of a few samples was very low. This data is not valid and was excluded. For behavioural experiments, we excluded data points from animals that had misplaced cannulas or inefficient viral spread.
Replication	All technical replicates were successful reproduced.
Randomization	For molecular profilling , naive mice of 9-12 weeks old C56/BL6 male mice were assigned randomly to experimental groups. For viral manipulation animal behavioral experiments in which 9-12 weeks old C56/BL6 cannulated male mice underwent fear conditioning prior to injection of a lentiviral vector, mice were assigned to receive a virus containing either control or active shRNA based on their freezing score from the last CS of a 3 CS-US training protocol. There is natural variation in the level of freezing behaviour displayed, which is increased in animals which have undergone surgery; group assignments were made so that the average freezing score for each treatment group was as similar as possible, to avoid a risk of random variation in learning confounding the effect of the shRNA injection.
Blinding	For behavioral studies, no blinding to group allocation since the groups need to counter balanced based on fear condition score. During behavioral test, data was blinded captured and analyzed by full automatic analysis software. For IHC, FACS and Sequencing, the investigators were blind to group allocation during data collection and analysis.

Reporting for specific materials, systems and methods

We require information from authors about some types of materials, experimental systems and methods used in many studies. Here, indicate whether each material, system or method listed is relevant to your study. If you are not sure if a list item applies to your research, read the appropriate section before selecting a response.

Materials & experimental systems

n/a	Involved in the study
☐	☒ Antibodies
☐	☒ Eukaryotic cell lines
☒	☐ Palaeontology
☐	☒ Animals and other organisms
☒	☐ Human research participants
☒	☐ Clinical data

Methods

n/a	Involved in the study
☐	☒ ChIP-seq
☐	☒ Flow cytometry
☒	☐ MRI-based neuroimaging

Antibodies

Antibodies used

H3K4me3 (active motif Cat# 39915, lot:14013006); YY1 (Abcam Cat# ab38422, lot:GR118077-26) ; TFIIB (Santa Cruz Cat# SC-274X, lot: J0215); Pol II (Santa Cruz Cat# sc-899X, clone: N-20, lot:F1715); m6A (Active motif Cat# 61495, clone:17-3-4-1, lot:06116001); Mouse IgG (Santa Cruz Cat# SC-2025; lot:K1115); N6amt1 (Santa Cruz Cat# SC-83304, lot:H0384); N6amt2 (Santa Cruz Cat# SC-390240, clone: H-3, lot:B0813); NeuN-Alex 488 (Abcam Cat# ab190195, lot:316293-3); Arc-Alex 647 (Bioss Cat# BS-0385R-A647, lot:AG11207885); Beta-actin (Santa Cruz Cat#SC-69879 Clone:AC-15 Lot#K1715); Beta tubulin (Santa Cruz Cat# SC-55529 clone:G8 lot# A1011); Mouse IgG (Active motif Cat# 103533 lot# 31111003); Rabbit IgG (cell signaling Cat# 29293 lot# 7).

Validation

N6amt1 antibody were selected from Santa Cruz. antibody has been validated by using IgG for chIP experiment, and over expression of N6amt1 in HEK293t cells was used to verify the antibody (Suppl.Fig.15 F). Previous validated antibody has been selected for H3K4me3 (Jun et al., Nucl. Acids Res. 2015), YY1 (Song et al., PLOS one, 2009), TFIIB (Pan et al., Cell report, 2014) and RNA Pol II (Chaudhary et al., Nucl. Acids Res. 2016). To re-validate the antibody, we used equivalent amount of control normal rabbit IgG (Santa Cruz), Rabbit IgG (Cell signalling) and mouse IgG (Active motif) was used for non-specificity control. For NeuN-Alex 488 and Arc-Alex 647, we run non labeling control to selected cells that co-express NeuN and Arc.

Eukaryotic cell lines

Policy information about cell lines

Cell line source(s)

N2A cell lines: ATCC® CCL-131™

Authentication

since we only use the cell line to validate the knock down constructs, we have not authenticated the cell line.

Mycoplasma contamination

The cell line were tested for mycoplasma contamination, and no mycoplasma contamination was observed

Commonly misidentified lines
(See ICLAC register)

no commonly misidentified cell lines were used in this study

Animals and other organisms

Policy information about studies involving animals; ARRIVE guidelines recommended for reporting animal research

Laboratory animals

C57/Bl6J male age between 10-14 weeks

Wild animals

no wild animal used in this study

Field-collected samples

no Field-collected samples used in this study

Ethics oversight

All testing took place during the light phase in red-light-illuminated testing rooms following protocols approved by the Institutional Animal Care and Use Committee of the University of California, Irvine and by the Animal Ethics Committee of The University of Queensland. Animal experiments were carried out in accordance with the Australian Code for the Care and Use of Animals for Scientific Purposes (8th edition, revised 2013).

Note that full information on the approval of the study protocol must also be provided in the manuscript.

ChIP-seq

Data deposition

☒ Confirm that both raw and final processed data have been deposited in a public database such as GEO.

☒ Confirm that you have deposited or provided access to graph files (e.g. BED files) for the called peaks.

Data access links
May remain private before publication.

ftp://ftp-trace.ncbi.nlm.nih.gov/sra/review/SRP110529_20170705_073201_94e0b7097bece407207267f7787e3012

Files in database submission	Raw fastq files have been deposited at the Sequence Read Archive (accession SRP110529) and BioProject (accession PRJNA391201).
Genome browser session (e.g. UCSC)	http://software.broadinstitute.org/software/igv/

Methodology

Replicates	Three biological replicates of each group were used
Sequencing depth	We performed the paired-end reads alignment for N6amt1 chIP-seq, and The total counts in each sample were normalised to 20 million before comparison among samples.
Antibodies	N6amt1 antibody purchased from Santa Cruz. The catalog is SC-83304 and host is rabbit.
Peak calling parameters	The potential binding sites were kept if they met all of the following conditions: i) the sites were not located in the mm10 empirical blacklists, and ii) the normalized counts in all three biological replicates in one group were larger than that in its input sample, and the normalized counts in at least 2 replicates were more than 2-folds larger than its normalized input count.
Data quality	We performed the paired-end reads alignment against mouse reference genome (mm10) using BWA (v0.6.2). Samtools (v0.1.17) was then used to convert "SAM" files to "BAM" files, sort and index the "BAM" files, and remove duplicate reads (i.e. potential PCR duplicates). Reads with low mapping quality (<20) or reads that were not properly paired-end aligned to the mouse reference genome were excluded from the downstream analysis. These steps ensure that only high-quality alignments were used for the downstream peak calling step. MACS2 (version 2.1.1.20160309) was used to call peaks for each sample with the parameter setting "callpeak -t SAMPLE -c INPUT -f BAMPE --keep-dup=all -g mm -p 0.05 -B". Here, we used the parameter "--keep-dup=all" for peak calling as we had removed the duplicate reads in previous steps. From the MACS output, 66 peaks are at FDR 5% and above 5-fold enrichment. Peak summits identified by MACS2 from all samples were collected to generate a list of potential n6amt1 binding sites. Custom PERL script was then applied to parse the number of fragments (hereafter referred as counts) that cover the peak summit in each sample. Each pair of properly paired-end aligned reads covering the peak summit represents one count. The total counts in each sample were normalized to 20 million before comparison among samples. The potential binding sites were kept if they met all of the following conditions: i) the sites were not located in the mm10 empirical blacklists, and ii) the normalized counts in all three biological replicates in one group were larger than that in its input sample, and the normalized counts in at least 2 replicates were more than 2-folds larger than its normalized input count. These steps ensure that the peaks we identified are consistently enriched in IP samples compared to input samples across different biological replicates.
Software	MACS2 (version 2.1.1.20160309) was used to call peaks for each sample with the parameter setting "callpeak -t SAMPLE -c INPUT -f BAMPE --keep-dup=all -g mm -p 0.05 -B". Peak summits identified by MACS2 from all samples were collected to generate a list of potential binding sites. Custom PERL script was then applied to parse the number of fragments (hereafter referred as counts) that cover the peak summit in each sample.

Flow Cytometry

Plots

Confirm that:

☒ The axis labels state the marker and fluorochrome used (e.g. CD4-FITC).

☒ The axis scales are clearly visible. Include numbers along axes only for bottom left plot of group (a 'group' is an analysis of identical markers).

☒ All plots are contour plots with outliers or pseudocolor plots.

☒ A numerical value for number of cells or percentage (with statistics) is provided.

Methodology

Sample preparation	FACS sorted RNA-seq: Tissue was dissociated with FACS lysis buffer (final concentration: 0.32M Sucrose, 10mM pH8.0, 5mM , 3mM , 0.1mM EDTA, 1mM DTT, 0.3% Triton-X -100 and 100x PIC) into single cell suspension, then fixed with 1% formaldehyde for 5 mins, and stop by 0.125M Glycine. Then, cells were washed twice with cold 1xPBS to remove excessed formaldehyde and glycine. After incubating with blocking buffer (Final concentration: 10% normal goat serum, 5% BSA, 0.1% Triton-X-100 and 1XPIC) for half-hour, cells were double-labeled with Arc antibody (Bioss) in 1:20000 dilution per million cell and NeuN antibody (Abcam) in 1:20000 per million cells, together with DAPI (Thermofisher) in 1:2000. PBPT buffer was used for washing (twice each time) and resuspend into 500ul 1x PBS for FACS sorting. FACS was performed on a BD FACSArial (BD Science)
Instrument	BD FACSAria Cell Sorter and BD FACSAriaII Cell Sorter
Software	BD FACSAria software
Cell population abundance	The sorting is for enriching the activated neurons. 518 positive cells were selected from 50,000 events
Gating strategy	The conjugated antibodies were used in FACS experiment. To set up sorting gate, we used non-neuronal cells to step up the

Gating strategy gating. Then, the sorted cells were selected by double labeling of Arc-647 and NeuN-488 antibody

☒ Tick this box to confirm that a figure exemplifying the gating strategy is provided in the Supplementary Information.